Cell Reports

Cellular and humoral functional responses after BNT162b2 mRNA vaccination differ longitudinally between naive and subjects recovered from COVID-19

Graphical abstract

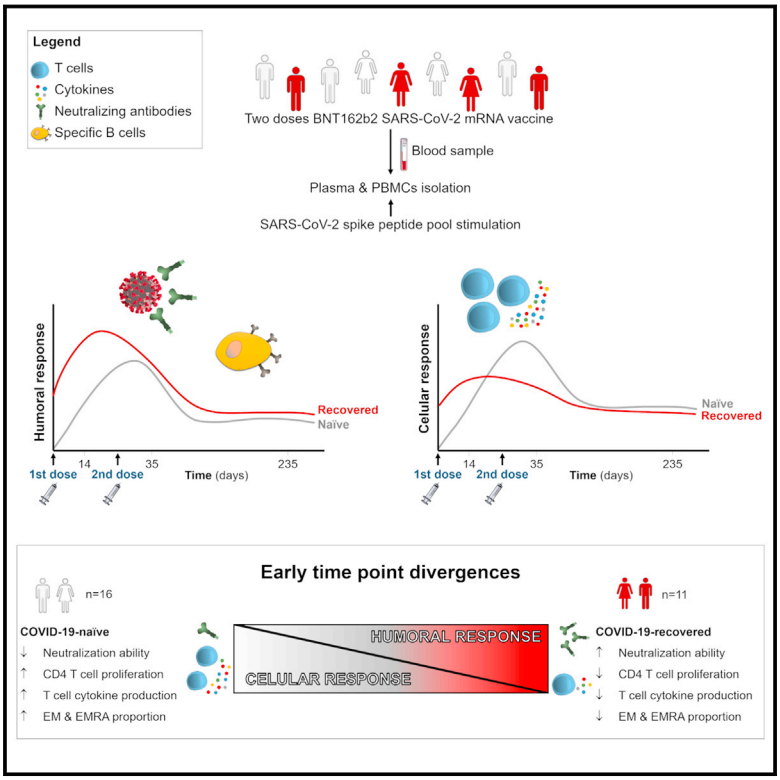

Highlights

- History of SARS-CoV-2 infection affects longitudinal responses to BNT162b2 vaccine
- Lower humoral but enhanced cellular responses early after vaccine in naive subjects
- Comparable humoral and cellular responses almost 8 months after vaccination
- Similar S-specific B cells late after vaccine in those naive and recovered from COVID-19

Authors

Roberto Lozano-Rodríguez, Jaime Valentín-Quiroga, José Avendaño-Ortiz, ..., Luis A. Aguirre, Carlos del Fresno, Eduardo López-Collazo

Correspondence

carlos.delfresno.sanchez@idipaz.es (C.d.F.), elopezc@salud.madrid.org (E.L.-C.)

In brief

Lozano-Rodríguez et al. show that naive subjects have enhanced SARS-CoV-2 spike-specific T reactions but reduced humoral-specific responses compared with individuals recovered from COVID-19. However, almost 8 months after vaccination, comparable specific responses are observed with equivalent levels of SARS-CoV-2-specific B cells and neutralizing antibodies.

Lozano-Rodríguez et al., 2022, Cell Reports *38*, 110235
January 11, 2022
https://doi.org/10.1016/j.celrep.2021.110235

CellPress

Cell Reports

CellPress
OPEN ACCESS

Report

Cellular and humoral functional responses after BNT162b2 mRNA vaccination differ longitudinally between naive and subjects recovered from COVID-19

Roberto Lozano-Rodríguez,[1,2,11] Jaime Valentín-Quiroga,[1,2,11] José Avendaño-Ortiz,[1,2,11] Alejandro Martín-Quirós,[3] Alejandro Pascual-Iglesias,[1,2] Verónica Terrón-Arcos,[1,2] Karla Montalbán-Hernández,[1,2] José Carlos Casalvilla-Dueñas,[1,2] Marta Bergón-Gutiérrez,[1,2] José Alcamí,[4] Javier García-Pérez,[4] Almudena Cascajero,[4] Miguel Ángel García-Garrido,[3] Álvaro del Balzo-Castillo,[1,3] María Peinado,[3] Laura Gómez,[3] Irene Llorente-Fernández,[5] Gema Martín-Miguel,[6] Carmen Herrero-Benito,[3] José Miguel Benito,[7,8] Norma Rallón,[7,8] Carmen Vela-Olmo,[9] Lissette López-Morejón,[9] Carolina Cubillos-Zapata,[1,2,10] Luis A. Aguirre,[1,2] Carlos del Fresno,[1,2,*] and Eduardo López-Collazo[1,2,10,12,*]

[1]The Innate Immune Response Group, IdiPAZ, La Paz University Hospital, Madrid, Spain
[2]Tumor Immunology Laboratory, IdiPAZ, La Paz University Hospital, Madrid, Spain
[3]Emergency Department and Emergent Pathology Research Group, IdiPAZ La Paz University Hospital, Madrid, Spain
[4]AIDS Immunopathogenesis Unit, National Microbiology Centre, Instituto de Salud Carlos III, Madrid, Spain
[5]Intensive Care Unit, Infanta Cristina University Hospital, Parla, Madrid, Spain
[6]Pediatric Intensive Care Unit, 12 de Octubre University Hospital, Madrid, Spain
[7]HIV and Viral Hepatitis Research Laboratory, Instituto de Investigación Sanitaria Fundación Jiménez Díaz, Universidad Autónoma de Madrid (IIS-FJD, UAM), Madrid, Spain
[8]Hospital Universitario Rey Juan Carlos, Móstoles, Spain
[9]Eurofins-Ingenasa, Madrid, Spain
[10]CIBER of Respiratory Diseases (CIBERES), Madrid, Spain
[11]These authors contributed equally
[12]Lead contact
*Correspondence: carlos.delfresno.sanchez@idipaz.es (C.d.F.), elopezc@salud.madrid.org (E.L.-C.)
https://doi.org/10.1016/j.celrep.2021.110235

SUMMARY

We have analyzed BNT162b2 vaccine-induced immune responses in naive subjects and individuals recovered from coronavirus disease 2019 (COVID-19), both soon after (14 days) and later after (almost 8 months) vaccination. Plasma spike (S)-specific immunoglobulins peak after one vaccine shot in individuals recovered from COVID-19, while a second dose is needed in naive subjects, although the latter group shows reduced levels all along the analyzed period. Despite how the neutralization capacity against severe acute respiratory syndrome coronavirus 2 (SARS-CoV-2) mirrors this behavior early after vaccination, both groups show comparable neutralizing antibodies and S-specific B cell levels late post-vaccination. When studying cellular responses, naive individuals exhibit higher SARS-CoV-2-specific cytokine production, $CD4^+$ T cell activation, and proliferation than do individuals recovered from COVID-19, with patent inverse correlations between humoral and cellular variables early post-vaccination. However, almost 8 months post-vaccination, SARS-CoV-2-specific responses are comparable between both groups. Our data indicate that a previous history of COVID-19 differentially determines the functional T and B cell-mediated responses to BNT162b2 vaccination over time.

INTRODUCTION

Severe acute respiratory syndrome coronavirus 2 (SARS-CoV-2) infection and its associated pathology, coronavirus disease 2019 (COVID-19), have had an enormous impact on healthcare systems worldwide and still constitute a challenge. Several vaccines have been authorized for emergency use by both the US Food and Drug Administration (FDA) and the European Medicines Agency (EMA). Among them, the BNT162b2 messenger RNA (mRNA) vaccine has been widely used following an accelerated two-dose vaccination schedule, which has exhibited specific humoral and cellular responses in 95% of individuals (Polack et al., 2020).

A number of studies have suggested a strong spike-specific antibodies generation by individuals recovered from COVID-19 after a first vaccine shot and that the second dose appears to be redundant (Ebinger et al., 2021; Gobbi et al., 2021; Levi et al., 2021; Prendecki et al., 2021a). In contrast, a second dose seems to be needed for a strong immunization in naive subjects (Ebinger et al., 2021; Levi et al., 2021; Mulligan et al., 2020; Walsh et al., 2020). Besides, the effect of this mRNA vaccine on spike-specific T cell responses has gained much attention (Ni et al.,

2020; Prendecki et al., 2021b; Sasikala et al., 2021). In this regard, to understand the cellular responses generated after vaccination, considering previous SARS-CoV-2 exposure is crucial for future adjustments in vaccination regimes.

Some reports are warning about the waning of the BNT162b2-vaccine-induced protection a few months after vaccination despite still showing a robust efficacy against suffering from COVID-19 (Chemaitelly et al., 2021; Goldberg et al., 2021). This wane has been linked to a decay in the levels of SARS-CoV-2-specific neutralizing antibodies (Bayart et al., 2021; Doria-Rose et al., 2021), although neither the role of SARS-CoV-2 spike-specific T (Guerrera et al., 2021) and B (Turner et al., 2021) cells is fully understood nor the relationship between both humoral and cellular responses triggered by COVID-19 vaccines against (re)infection.

Herein, we aimed to evaluate the immune responses triggered by immunization with the BNT162b2 vaccine in a cohort of naive subjects and individuals recovered from COVID-19. Both humoral and cellular responses were thoroughly analyzed using blood samples taken before vaccination, after the first dose, 14 days, and almost 8 months after the vaccination regime was completed. Our data indicated that previous SARS-CoV-2 exposure conditioned early responses post-vaccination, as naive subjects showed enhanced SARS-CoV-2 spike-specific $CD4^+$ T cells but reduced humoral spike-specific responses compared with individuals recovered from COVID-19. However, almost 8 months after vaccination, comparable humoral and cellular responses were observed in both groups, importantly, with equivalent levels of SARS-CoV-2-specific memory B cells and neutralizing antibodies. Therefore, our findings suggest that previous exposure to the virus determines early functional T and B cell-mediated responses to BNT162b2 vaccination. However, both naive subjects and individuals recovered from COVID-19 show comparable memory SARS-CoV-2-specific immunity almost 8 months after vaccination.

RESULTS

Humoral responses triggered after vaccination show specific kinetics in naive subjects and individuals recovered from COVID-19

Following the BNT162b2 vaccination strategy recommended by both the FDA and the EMA, a total of 27 individuals were vaccinated with a two-dose regime administrated 21 days apart. Of them, 16 had not been previously exposed to SARS-CoV-2 coronavirus (naive), while 11 were reported as having recovered from COVID-19 (Table S1). For all participants, four blood samples were taken: 5 days before the first dose (sample 0), 14 days after the first dose (sample 1), 14 days after the second dose (sample 2), and a final long-term sample collected 230 days (almost 8 months) after the second dose (sample 3) (Figure 1A).

We first analyzed the levels of SARS-CoV-2-specific plasma immunoglobulins. One vaccination dose induced the presence of both anti-spike S1 immonoglobulin A (IgA) and anti-receptor binding domain (RBD) IgAs, whose levels were further boosted by the second immunization dose in naive individuals (Figure 1B). Although subjects recovered from COVID-19 showed higher levels of IgA than naive participants after the first dose, the concentrations after the second vaccination shot were comparable between both groups and, again, slightly higher in subjects recovered from COVID-19 after almost 8 months post-vaccination (sample 3) (Figure 1B). The analysis of IgGs (anti-spike S1, anti-RBD, and anti-full spike) in sample 0 confirmed that the subjects recovered from COVID-19 had been previously exposed to SARS-CoV-2, and these participants showed higher levels of specific IgGs than naive individuals throughout the observation period (Figure 1C). It is noteworthy that the titers of all the analyzed antibodies dropped in sample 3, but individuals recovered from COVID-19 maintained slightly higher levels (Figures 1B and 1C).

Beyond the Ig concentrations, we evaluated the neutralization capacity of plasma against the spike antigen. The neutralization capacity was measured using a competitive immunoassay. In naive individuals, two doses were required to induce neutralizing antibodies, whereas in recovered individuals, one dose induced high neutralization titers. Of note, after a second dose, subjects recovered from COVID-19 further increased their neutralization activity, which was higher than in naive individuals 14 days after full vaccination (Figure 1D). Note that, although the neutralization capacity was still measurable, the neutralizing antibodies dropped dramatically in sample 3. Importantly, this neutralization ability was similar between naive subjects and individuals recovered from COVID-19 at this long-term post-vaccination time (Figure 1D). To further characterize the differential neutralization capacity conditioned by previous exposure to SARS-CoV-2, a functional assay based on the neutralization of a pseudovirus expressing the spike protein of SARS-CoV-2 was done. We accomplished this analysis in sample 2, the first one where both naive subjects and individuals recovered from COVID-19 showed neutralizing activity. This analysis confirmed that individuals recovered from COVID-19 exhibited a better neutralizing capacity (Figure S1A). Altogether, these data indicated a differential expression pattern of humoral responses between naive individuals and subjects recovered from COVID-19 over time post-vaccination (Figure 1E).

Next, we focused on circulating B cell-derived populations because of their role in humoral responses. Based on a fluorescence-activated cell sorting (FACS) panel of 39 extracellular markers and an unsupervised uniform manifold approximation and projection (UMAP) dimensional reduction followed by manual gating, we identified canonical cell subsets in peripheral blood mononuclear cells (PBMCs) (Figure 1F). Again, we performed this analysis in sample 2, where naive subjects and individuals recovered from COVID-19 showed neutralizing activity (Figure 1D). An overall analysis of B cells differentiated up to 6 different subpopulations in naive subjects and patients recovered from COVID-19 (Figure 1G). The UMAP analysis of human leukocyte antigen (HLA)-DR, IgD, IgM, and IgG expressions suggested no major changes between these two groups (Figure 1H), which was confirmed by quantitative assessments (Figure S1B–S1H). The same multiparametric approach was applied to study circulating T cells, showing that the populations' distribution and activation markers' expression were comparable between naive subjects and individuals recovered from COVID-19 except for a slight increase in $CD4^+$ T regulatory cells (Figure S2).

CellPress
OPEN ACCESS

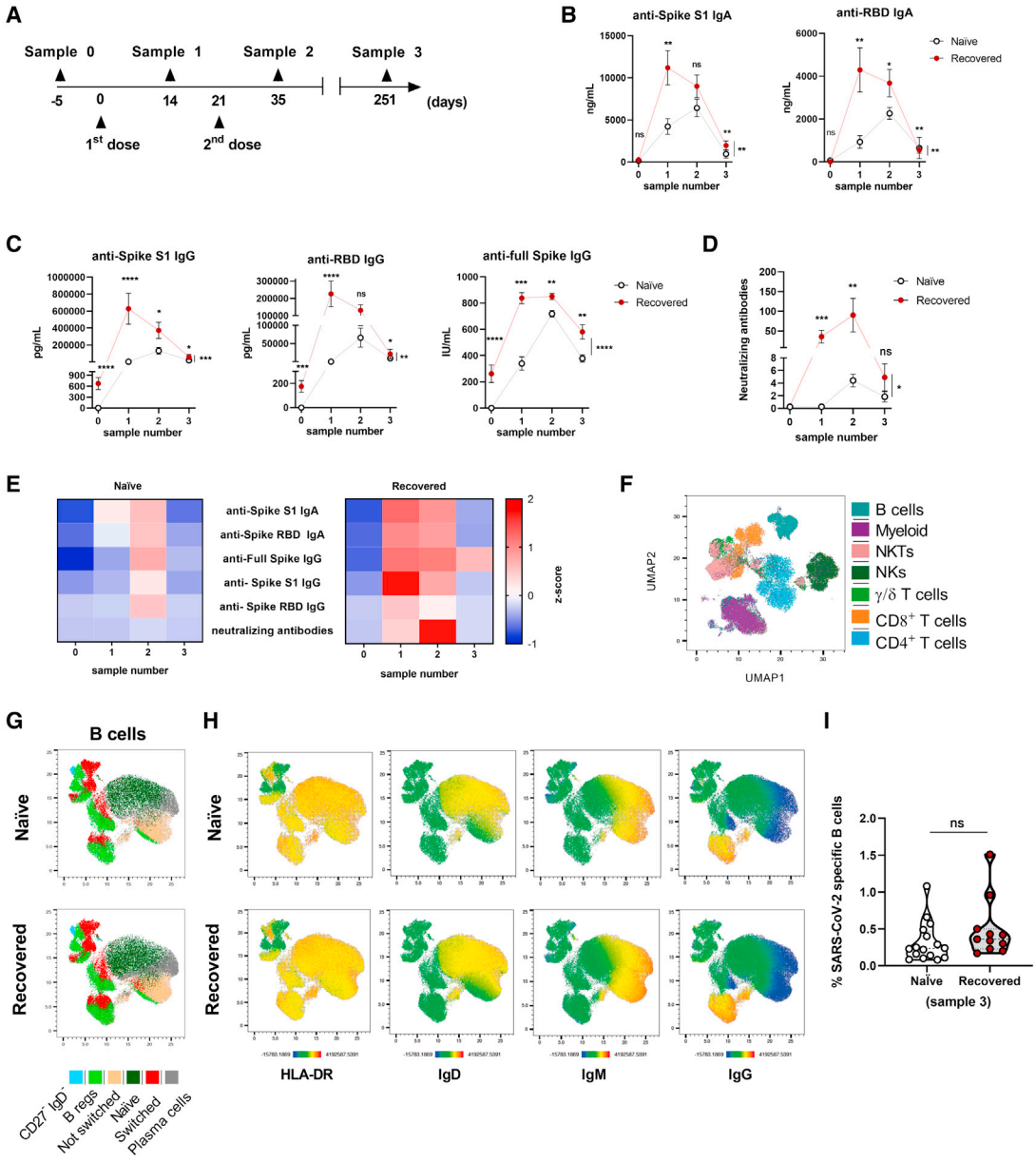

Figure 1. SARS-CoV-2 spike-specific humoral response following BNT162b2 mRNA vaccination in naive subjects and individuals recovered from COVID-19

(A) Experimental design. Blood samples were collected 5 days before BNT162b2 mRNA vaccination (sample 0), 14 days after the first dose (sample 1), and 14 days (sample 2) and 230 days (sample 3) after the second dose.

(B) Concentrations of plasma anti-spike S1 IgA (left panel) and anti-receptor binding domain (RBD) IgA (right panel) antibodies.

(C) Concentrations of plasma anti-spike S1 IgG (left panel), anti-RBD IgG (central panel), and anti-full spike IgG (right panel) antibodies.

(D) Concentration of neutralizing antibodies in plasma by means of a competitive assay; 10^8/free anti-spike signal is depicted.

(E) Heatmap of *Z* score of IgA, IgG, and anti-spike neutralizing antibodies.

(F) Uniform manifold approximation and projection (UMAP) of peripheral blood mononuclear cells (PBMCs) followed by manual gating to identify the indicated populations.

(G) UMAP of B cells followed by manual gating to identify the indicated populations in sample 2.

(H) UMAP clustering expressions of HLA-DR, IgD, IgM, and IgG on B cells.

(I) Frequency of SARS-CoV-2 spike-specific B cells in gated $CD19^+$ cells in sample 3.

(B, C, D, and I) Data shown as mean ± SEM (ns, not significant; *$p < 0.05$; **$p < 0.01$; ***$p < 0.001$; ****$p < 0.0001$). Unpaired Student's t test in samples 0, 1, 2, or 3.

(B, C, and D) Two-way ANOVA analyzing the time course (denoted by vertical bar, |). n = 16 naive, n = 11 recovered from COVID-19.

See also Figures S1, S2, and S3A.

Considering the lack of differences in the levels of neutralizing antibodies between naive subjects and individuals recovered from COVID-19 almost 8 months after complete vaccination (sample 3; Figure 1D), we decided to analyze the levels of SARS-CoV-2 spike-specific B cells in this long-term time point (Figure S3A). Remarkably, all of the participants showed SARS-CoV-2 spike-specific B cells, with comparable levels between groups (Figure 1I).

Naive individuals show enhanced SARS-CoV-2-specific T cell lymphoproliferative responses early after vaccination but are similar to those recovered from COVID-19 at later time points

To explore whether previous exposure to SARS-CoV-2 could modulate specific cellular responses against this coronavirus in fully vaccinated individuals, PBMCs from both naive and recovered subjects were *ex vivo*-exposed to a peptide pool covering the SARS-CoV-2 spike protein, henceforth called the S-peptide (Figure 2A). First, we analyzed the presence of several chemokines and cytokines in culture supernatants after this *ex vivo* stimulation for 5 days. The production of both CCL-2 and CXCL10 was induced by the SARS-CoV-2 spike peptide pool except for CCL-2 in individuals recovered from COVID-19 almost 8 months post-vaccination (Figure 2B). However, only naive individuals showed a robust induction of most of the cytokines analyzed (interleukin [IL]-2, IL-4, IL-6, IL-10, and tumor necrosis factor alpha [TNFα]), although this S-peptide-specific response in naive subjects was exclusive to sample 2 (Figure 2C). Interestingly, interferon (IFN)-γ expression showed a specific pattern, mirroring CCL2 production (Figures 2B and 2C).

To further examine this differential outcome, cytokine production was analyzed by intracellular FACS staining. The expression of IL-2, TNFα, IFN-γ, and granzyme B were consistently induced in $CD4^+$ T cells after *ex vivo* stimulation with the S-peptide pool in both naive subjects and individuals recovered from COVID-19 early after vaccination (sample 2) (Figures 2D and S4), with less robust responses in $CD8^+$ T cells. However, more than 7 months after vaccination (sample 3), this SARS-CoV-2-specific response was negligible in both groups (Figures 2D and S4).

Interestingly, the analysis of the intracellular cytokine production increment induced by SARS-CoV-2 spike antigen *ex vivo* stimulation showed a much more intense induction of IL-2 in both $CD4^+$ and $CD8^+$ T cells from naive subjects than from individuals recovered from COVID-19 early after vaccination (sample 2) (Figure 2E). Considering the crucial role of IL-2 in the lymphoproliferative capacity of $CD4^+$ T cells, we decided to analyze this function. Proliferation ability was explored based on carboxyfluorescein succinimidyl ester (CFSE) dilution of total PBMCs after *ex vivo* stimulation with the S-peptide pool. Both $CD4^+$ and $CD8^+$ T cells proliferated in response to the spike antigen in naive subjects and individuals recovered from COVID-19, although with an apparent stronger effect on $CD4^+$ T cells from naive subjects (Figure 2F). The increment of proliferation between SARS-CoV-2 spike-antigen-stimulated and non-stimulated PBMCs confirmed a more powerful $CD4^+$ lymphoproliferative activity in naive subjects than in individuals recovered from COVID-19, specifically, early after vaccination (sample 2) (Figure 2G).

These data suggest a strong SARS-CoV-2 spike-specific T cell response early after vaccination in naive subjects (but not in COVID-19-recovered individuals) that declines over time.

SARS-CoV-2-specific effector memory T cell enhanced responses in naive individuals decline along the timeline

Next, we dissected the SARS-CoV-2 spike-specific T cell responses. First, we analyzed the phenotype of both proliferative ($CFSE^{dim}$) and non-proliferative ($CFSE^{bright}$) $CD4^+$ T cells after antigen-specific stimulation (Figure S3B). As expected, this challenge induced the transition from a naive to effector memory (EM) phenotype in proliferated $CD4^+$ T cells (Figures 3A and 3B). Of note, early after vaccination (sample 2), an increase in the frequency of EM re-expressing CD45RA (EMRA) cells was observed, while almost 8 months after vaccination (sample 3), a significant central memory (CM) response was induced (Figures 3A and 3B). Interestingly, the study of these populations in terms of proliferative capacity showed that previous exposure to SARS-CoV-2 had no impact on these transitions along the timeline (Figure 3C). Although in a less robust way, similar behaviors were observed for $CD8^+$ T cells (Figures S5A–S5C).

We next analyzed intracellular cytokine production in $CD4^+$ T cell subpopulations induced by *ex vivo* SARS-CoV-2 spike peptide pool stimulation. A consistent IL-2 production was observed in naive individuals early after vaccination (sample 2) that was maintained in effector populations (EMRA and EM) in the long term (sample 3) (Figure 3D). However, $CD4^+$ T cells from subjects recovered from COVID-19 did not respond to the SARS-CoV-2 spike peptide pool stimulation at any time (Figure 3D). In line with previous observations, naive individuals showed a stronger increment of IL-2 production in the EMRA and EM population than did subjects recovered from COVID-19 early after vaccination that declined almost 8 months post-vaccination (Figure 3E). Again, despite a less robust response after antigen-specific stimulation, a similar IL-2 expression pattern was observed in $CD8^+$ T cells (Figures S5D and S5E).

These data indicated that previous infections of SARS-CoV-2 dampened T EM cellular responses early after a complete BNT162b2 vaccination. However, almost 8 months post-vaccination, the SARS-CoV-2 spike-specific T responses were comparable between naive subjects and individuals recovered from COVID-19.

Humoral and cellular activation features are inversely correlated early after vaccination

Based on the differential behavior of SARS-CoV-2 spike-specific humoral and cellular responses between naive subjects and individuals recovered from COVID-19, we explored whether these features could identify subjects belonging to these two groups, in an unsupervised manner, in samples 2 and 3. To address this question, we performed a clustering analysis based on the different immunological variables studied in this work (Figure 4A). This algorithm generated a clearer discrimination between naive subjects and individuals recovered from COVID-19 in sample 2 than in sample 3 (Figure 4A).

Next, we depicted the correlation between the analyzed variables once they were classified based on their functionality. Along

CellPress
OPEN ACCESS

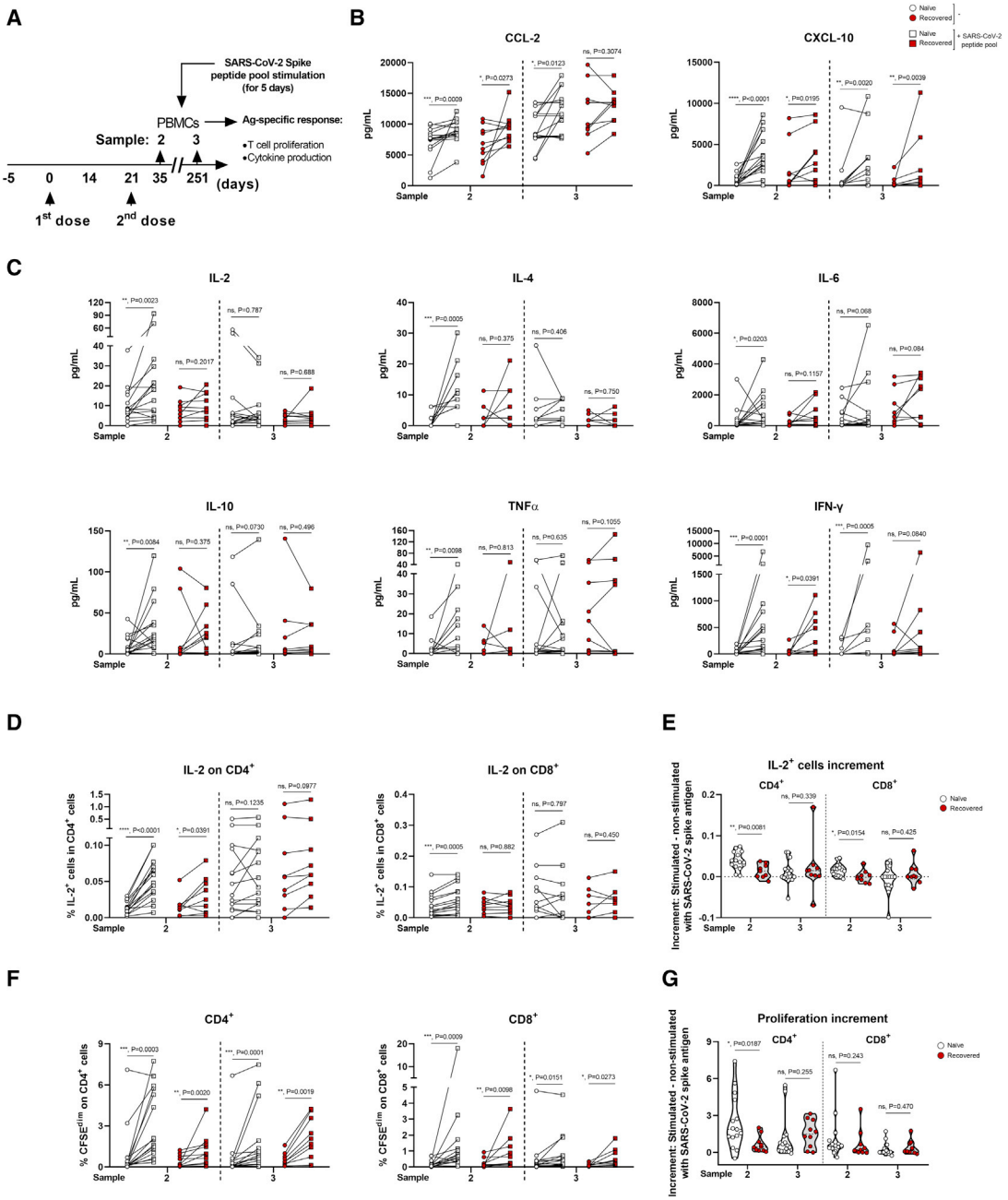

Figure 2. SARS-CoV-2 spike-specific cellular *ex vivo* response following BNT162b2 mRNA vaccination in naive subjects and individuals recovered from COVID-19

(A) Experimental design of the T cell cellular response *ex vivo* in PBMCs in samples 2 and 3 after stimulation with SARS-CoV-2 spike peptide pool.

(B) CCL-2 and CXCL10 chemokines production.

(C) IL-2, IL-4, IL-6, IL-10, TNFα, and IFNγ production.

(D) Percentage of IL-2$^+$ cells in CD4$^+$ (left panel) and CD8$^+$ (right panel) T cells.

(E) Increment of IL-2$^+$ cells comparing SARS-CoV-2 spike peptide pool-stimulated and non-stimulated CD4$^+$ and CD8$^+$ T cells.

(F) Frequency of proliferative (CFSE^{dim}) CD4$^+$ and CD8$^+$ T cells.

(G) Increment of proliferation comparing SARS-CoV-2 spike peptide pool-stimulated and non-stimulated CD4$^+$ and CD8T cells.

(B–G) Each dot represents an individual. (B–D and F) Paired Student's t test (ns, not significant; *p < 0.05; **p < 0.01; ***p < 0.001; ****p < 0.0001). (E and G) Mann Whitney test (ns, not significant; *p < 0.05; **p < 0.01). n = 16 naive, n = 11 recovered from COVID-19.

See also Figure S4.

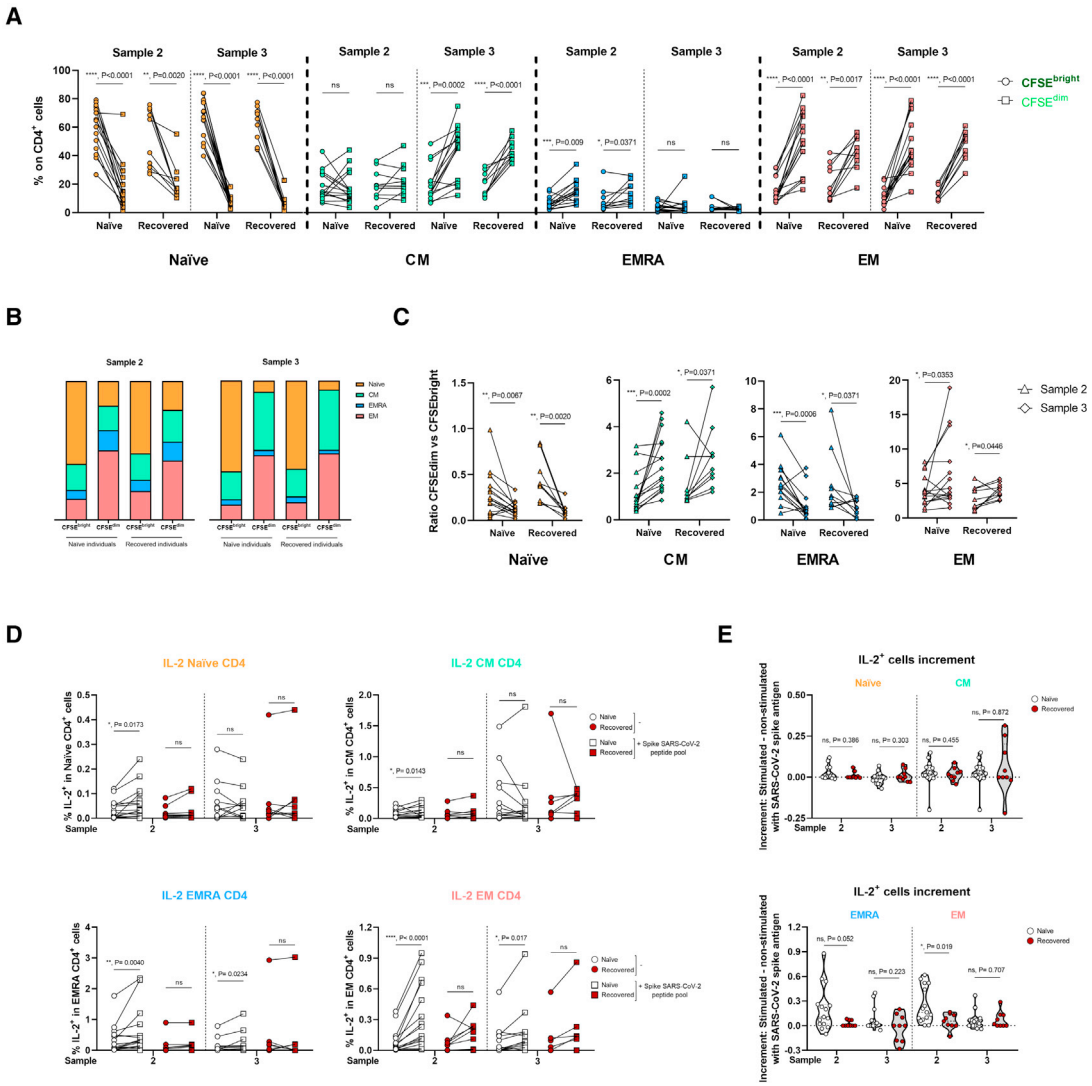

Figure 3. Memory populations in SARS-CoV-2 spike-specific CD4$^+$ T cells following BNT162b2 mRNA vaccination in naive subjects and individuals recovered from COVID-19

(A and B) PBMCs were labeled with CFSE and stimulated with SARS-CoV-2 spike peptide pool for 5 days. CD4$^+$ T cells were classified according to their proliferative response in samples 2 and 3. Memory subpopulations were analyzed (naive; CM, central memory; EMRA, effector memory cells re-expressing CD45RA; EM, effector memory). Frequencies (A) and mean distribution (B) of memory populations in proliferative (○; CFSE^{dim}) and non-proliferative (□; CFSE^{bright}) CD4$^+$ T cells.

(C) Proliferative (CFSE^{dim}) versus non-proliferative (CFSE^{bright}) ratio of CD4$^+$ T cell memory populations in samples 2 (Δ) and 3 (◇).

(D) Frequency of IL-2$^+$ cells in gated naive, CM, EMRA, and EM CD4$^+$ T cells stimulated or not with SARS-CoV-2 spike peptide pool.

(E) Increment of frequencies of IL-2$^+$ cells comparing SARS-CoV-2 spike pool-stimulated and non-stimulated CD4$^+$ T cell subpopulations.

(A, C–E) Each dot represents an individual. (A, C, and D) Paired Student's t test (ns, not significant; *p < 0.05; **p < 0.01; ***p < 0.001; ****p < 0.0001). (E) Mann Whitney test (ns, not significant; *p < 0.05). n = 16 naive, n = 11 recovered from COVID-19.

See also Figure S3B, S3C, and S5.

these lines, humoral parameters quantified in plasma were confronted to the cellular response after *ex vivo* cellular stimulation with SARS-CoV-2 spike peptide pool (Figure 4B). This representation suggested inverse correlations early after vaccination (sample 2) between humoral and cellular responses, particularly IgG production and neutralization capacity of SARS-CoV-2 spike-specific pro-inflammatory cytokine (CCL2, CXCL10, IFNγ, and IL-2) production and CD4$^+$ T cell proliferation (Figure 4B). However, these correlations were attenuated more than 7 months after vaccination (sample 3) (Figure 4B). The analysis of these correlations confirmed the statistically significant inverse association between Ig-based and cellular responses such as CD4$^+$ T cell proliferation or IL-2 production in sample 2 (Figure 4C). However, no significant correlations were found between these variables in sample 3 (Figure 4C). Altogether, these analyses revealed that early after a complete vaccination regimen with BNT162b2, differential humoral

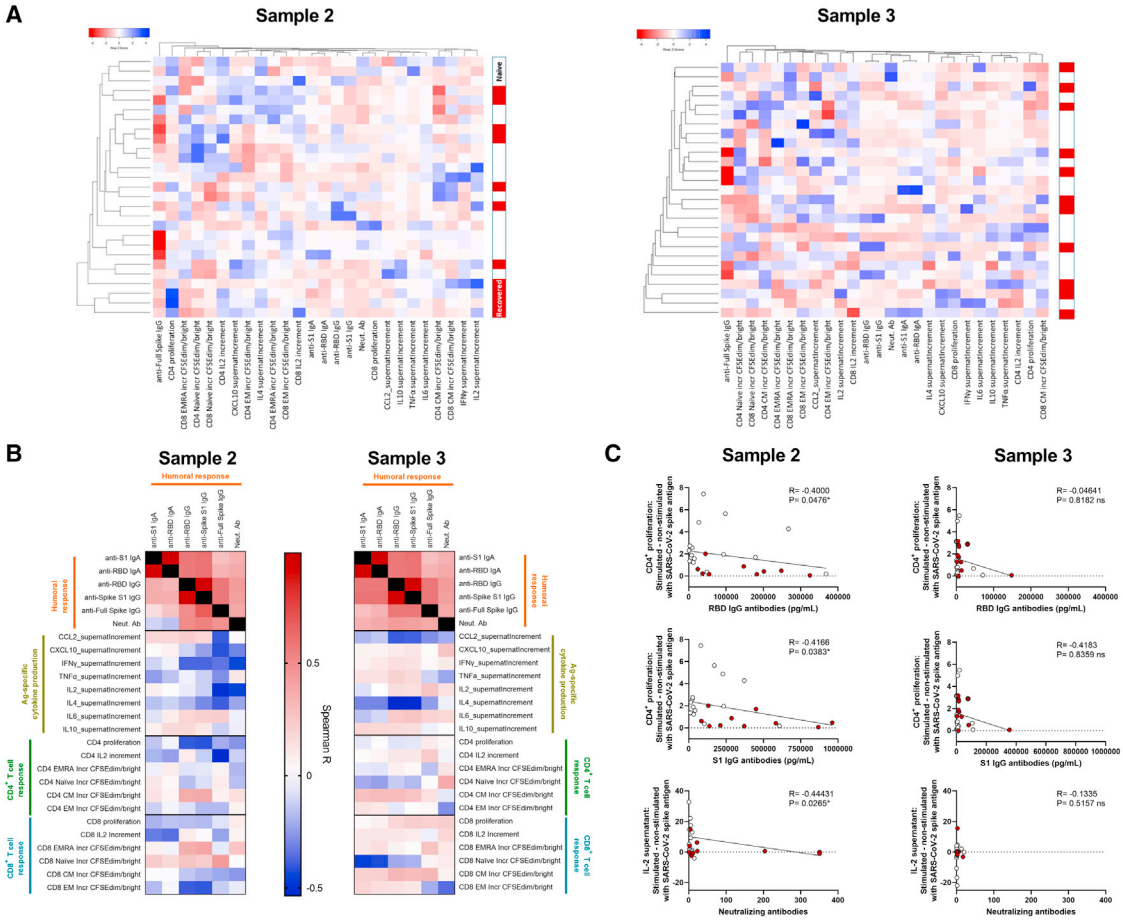

Figure 4. Differential SARS-CoV-2 spike-specific humoral and cellular responses between naive subjects and individuals recovered from COVID-19 after vaccination

(A) Heatmap analysis of main humoral and cellular variables of SARS-CoV-2 spike-specific responses. This algorithm showed differential clustering distribution between naive subjects and individuals recovered from COVID-19.

(B) Spearman correlation matrix heatmap of the main humoral and cellular variables of SARS-CoV-2 spike-specific responses grouped by functionality.

(C) Spearman correlations between different SARS-CoV-2 spike-specific humoral and cellular responses. Top: ratio of $CD4^+$ T cells proliferation versus titers of RBD IgG antibodies; middle: ratio of $CD4^+$ T cells proliferation versus S1 IgG antibodies; bottom: IL-2 production in supernatants versus titers of neutralizing antibodies. R, Spearman's rank correlation coefficient. p value in Spearman correlation test (ns, not significant; *$p < 0.05$). White dots represent naive individuals; red dots represent subjects recovered from COVID-19. n = 16 naive, n = 11 recovered from COVID-19.

and cellular responses were triggered between naive subjects and individuals recovered from COVID-19 almost eight months after vaccination, both responses were comparable between both groups.

DISCUSSION

The generation of mRNA COVID-19 vaccines such as mRNA-1273 (Baden et al., 2021) and BNT162b2 (Polack et al., 2020) represents a revolution in vaccinology and is one of the key pillars of humanity's eventual success against the pandemic caused by the SARS-CoV-2 infection. These vaccines are based on a lipid-nanoparticle-encapsulated mRNA encoding the full-length spike protein of the SARS-CoV-2 virus (Corbett et al., 2020; Walsh et al., 2020). The BNT162b2 vaccine was the first COVID-19 vaccine approved for emergency use by both the FDA and the EMA. This approval was based on the results of a clinical trial declaring an efficacy of 95% in preventing COVID-19 after a two-dose regime 21 days apart (Polack et al., 2020). Since then, a global vaccination campaign began aiming to face off the pandemic.

It is worth noting that a medical history of COVID-19 was an exclusion criterion to be enrolled in the above-mentioned clinical trial (Polack et al., 2020). Therefore, the potential effect of a previous infection with SARS-CoV-2 was not anticipated. Here, we have performed a broad analysis of both humoral and cellular responses triggered by BNT162b2 vaccination by comparing naive subjects and individuals recovered from COVID-19 along a timeline after receiving the complete vaccine regime. We performed a massive phenotypic study of PBMCs after vaccination, but more importantly, it was accompanied by the analysis of functional immunological capabilities such as antibody neutralization and

T cell activation and proliferation in response to specific SARS-CoV-2 spike antigens. Notably, our analysis covers responses after only one vaccine dose but also early (14 days) and late (more than 7 months) responses after the complete two-dose vaccination regime.

Previous studies addressing differential responses between naive subjects and individuals recovered from COVID-19 have focused on the analysis of specific antibodies as a subrogated of vaccine efficacy. In phase 1/2 studies, mRNA immunization with BNT162b2 showed that two doses were requested to elicit high titers of neutralizing antibodies in naive individuals; in contrast, in recovered patients, the first immunization acted as a booster, thus inducing neutralization titers higher than those observed after the full immunization of naive patients (Mulligan et al., 2020; Walsh et al., 2020). Along the same lines, a pioneer study indicated that individuals with a previous SARS-CoV-2 infection generated stronger humoral responses than infection-naive subjects after just a single dose of the BNT162b2 vaccine (Prendecki et al., 2021a). These findings were confirmed in a cohort of volunteers that received either the BNT162b2 or the mRNA-1273 vaccine (Krammer et al., 2021) but also in individuals receiving only one shot of the vaccine based on the SARS-CoV-2 spike protein-expressing adenovirus (Sasikala et al., 2021; Voysey et al., 2021). Nevertheless, follow-up studies showed that anti-spike SARS-CoV-2 IgGs titers were comparable between naive subjects and individuals recovered from COVID-19 after 11 to 21 days of the complete two-dose regime (Ebinger et al., 2021; Levi et al., 2021). Of note, our data on early humoral responses support these findings. We also observed that antibody levels and the neutralizing capacity of plasma from individuals recovered from COVID-19 were higher than that of naive subjects early after vaccination (samples 1 and 2), an effect suggested but not fully analyzed in a previous study (Gobbi et al., 2021). However, more than 7 months after vaccination, individuals recovered from COVID-19 still showed higher antibody titers but comparable neutralizing antibodies to naive subjects. These data highlight the need to discriminate between antibody titers and neutralizing capacity. In addition, the analysis of this neutralizing capacity against specific SARS-CoV-2 variants of concern (Carreño et al., 2021; Noori et al., 2021) would improve our understanding about the breadth of the vaccine-conferred protection.

The relevance of cellular responses after SARS-CoV-2 virus infection have been studied (Grifoni et al., 2020; Ni et al., 2020), but data regarding how previous exposure to SARS-CoV-2 impacts these immunogenic responses along the timeline after vaccination are still scarce. Memory B cell responses one week after vaccination were boosted in individuals recovered from COVID-19 after just one shot of the mRNA vaccine, while naive subjects required two doses to reach comparable memory B cell levels (Goel et al., 2021). This response mirrors the production of SARS-CoV-2 spike-specific antibodies early after vaccination, as previously discussed.

The analysis of the vaccine-induced humoral responses 7 months after the complete vaccination regime showed a drop in antibody titers in the long term, in accordance with other studies (Doria-Rose et al., 2021; Naaber et al., 2021), along with a marked decrease in the neutralizing capacity, reaching comparable low levels in both naive subjects and individuals recovered from COVID-19. Of note, these data do not necessarily indicate the lack of specific protection against the SARS-CoV-2 virus because, in line with other studies (Ciabattini et al., 2021; Turner et al., 2021), we detected circulating SARS-CoV-2 spike protein-specific B cells even more than 7 months after full vaccination. Importantly, the levels of these B cells were comparable between naive subjects and participants recovered from COVID-19. Considering that SARS-CoV-2 spike-specific memory B cells showed a switch to an anti-RBD neutralizing phenotype (Sokal et al., 2021), it is tempting to speculate that long-term protection already documented for the BNT162b2 vaccine (Thomas et al., 2021) is warranted, based at least in part on the restimulation of these cells during a SARS-CoV-2 reinfection. Future studies will shed light on the efficacy of this specific protective mechanism.

In our study, we analyzed SARS-CoV-2 spike-specific responses in T cells after restimulation with a peptide pool covering this antigen. This assay showed a differential response between naive subjects and individuals recovered from COVID-19 early after vaccination, with a more pronounced activation of $CD4^+$ T cells in naive subjects. This was revealed by a higher induction of cytokine production and proliferation after restimulation, particularly in EM cells. The mechanistic implication of regulatory T cells (Tregs) in this effect (Campbell and Koch, 2011) deserves further studies, as we observed higher levels of this immunomodulatory population in individuals recovered from COVID-19 at this early time point after vaccination. Of note, high levels of SARS-CoV-2 spike-specific $CD4^+$ T cells correlate with a lower COVID-19 predisposition (Sattler et al., 2020), stressing the relevance of a robust cellular response. Of note, previously published data indicated a reduction of the SARS-CoV-2-specific T cell-mediated responses along the timeline after vaccination (Guerrera et al., 2021). Along these lines, we observed that T cell responses dropped to comparable levels in both naive subjects and individuals recovered from COVID-19.

Our data point toward boosted T cell responses in naive individuals early after complete BNT162b2 vaccination in a scenario of reduced humoral reactions such as lower SARS-CoV-2 spike-specific IgGs titers and neutralizing capabilities. This concerted response allowed an unsupervised clustering of naive subjects and individuals recovered from COVID-19 that anticipated inverse correlations between cellular and humoral immune responses. This is relevant, as it is known that cellular immunity may contribute to protection against SARS-CoV-2 infection if antibody responses are suboptimal (McMahan et al., 2021). Therefore, our data suggest that this differential mechanism could take place early after vaccination in naive individuals compared with in subjects recovered from COVID-19. However, more than 7 months after vaccination, humoral and cellular responses dropped similarly in both naive subjects and individuals recovered from COVID-19, showing no correlations. Still, memory SARS-CoV-2 spike-specific B cells were present at comparable levels in both groups, suggestive of an equivalent long-term protection mechanism (Ciabattini et al., 2021; Turner et al., 2021).

In summary, our data indicate that concerted humoral and cellular responses over time after vaccination should be considered to define vaccination regimes against COVID-19. This notion could apply to proposals such as the delay of the second vaccination dose (Kadire et al., 2021), the administration of just one shot to a population previously infected with SARS-CoV-2 (Goel et al., 2021), or of a third boosting dose (Mahase, 2021).

Limitations of the study

Sample size is a limitation of this study. Considering the high number of immune variables analyzed and their complexity, we decided to perform our study with a not-so-large but well-controlled cohort of participants. We believe that this approach allowed us to reach clear conclusions, but a multicentre cohort with a larger number of patients would be desirable. Furthermore, all stimulations and detections of SARS-CoV-2-specific responses have been performed against the original S-protein. The analysis of such responses against SARS-CoV-2 variants of concern would expand the relevance of our study. Finally, mechanistic studies would help to explain the divergent responses observed between naive subjects and individuals recovered from COVID-19.

STAR★METHODS

Detailed methods are provided in the online version of this paper and include the following:

- KEY RESOURCES TABLE
- RESOURCE AVAILABILITY
  - Lead contact
  - Material availability
  - Data and code availability
- EXPERIMENTAL MODEL AND SUBJECT DETAILS
  - Healthy health personnel volunteers and longitudinal samples
  - Culture conditions of primary and Vero E6 cells
- METHOD DETAILS
  - PBMCs isolation, storage and thawing procedure
  - Plasma collection
  - Algorithm for dimensionality reduction
  - Detection of anti-spike IgA and IgG SARS-CoV-2 antibodies
  - Detection of neutralization capacity of plasma against SARS-CoV-2 Spike antigen
  - Antibodies and immunophenotyping by flow cytometry
  - SARS-CoV-2 Spike-specific B cells detection
  - SARS-CoV-2 Spike-specific T cell proliferation assays and supernatant collection
  - Supernatant soluble cytokine quantification
  - PBMCs stimulation and intracellular cytokine staining
- QUANTIFICATION AND STATISTICAL ANALYSIS
  - Statistical analysis of biological data

SUPPLEMENTAL INFORMATION

Supplemental information can be found online at https://doi.org/10.1016/j.celrep.2021.110235.

ACKNOWLEDGMENTS

C.d.F., J.G.-P., and J.A. are supported by Instituto de Salud Carlos III (ISCII). We thank JM Ligos and Cytek Biosciences for their technical support. Research in E.L.-C.'s lab was supported by Fundación Familia Alonso, Santander Bank, Real Seguros, Fundación Mutua Madrileña, Fundación Uria, Fundación La Caixa, and Ayuntamiento de Madrid. This work is dedicated to the memory of Norma López-Collazo.

AUTHOR CONTRIBUTIONS

E.L.-C., C.d.F., R.L.-R., J.A.-O., and L.A.A. designed the study. E.L.-C. and C.d.F. wrote the manuscript. A.M.-Q., M.A.G.-G., A.d.B.-C., M.P., L.G., I.L.-F., G.M.-M., and C.H.-B. recruited the participants and collected the samples. R.L.-R., J.A.-O., J.V.-Q., K.M.-H., J.C.C.-D., M.B.-G., and V.T. performed the analysis and the immunological biomarkers quantification. J.M.B. and N.R. provided the know-how and critical reagents for the intracellular FACS staining. J.V.-Q. and C.d.F. performed the UMAP analysis. J.A., J.G.-P., A.C., C.V.-O., and L.L.-M. performed design and neutralization testing. A.P.-I. performed the clustering heatmap analysis. E.L.-C., C.d.F., R.L.-R., J.A.-O., J.V.-Q., C.C.-Z., and L.A.A. discussed the results. R.L.-R., J.A.-O., J.V.-Q., and L.A.A. performed a critical review of the manuscript. All authors read and agreed to submit the manuscript for publication.

DECLARATION OF INTERESTS

The authors declare no competing interests.

INCLUSION AND DIVERSITY

We worked to ensure gender balance in the recruitment of human subjects. We worked to ensure ethnic or other types of diversity in the recruitment of human subjects. We worked to ensure that the study questionnaires were prepared in an inclusive way. One or more of the authors of this paper self-identifies as an underrepresented ethnic minority in science. One or more of the authors of this paper self-identifies as a member of the LGBTQ+ community. One or more of the authors of this paper received support from a program designed to increase minority representation in science. The author list of this paper includes contributors from the location where the research was conducted who participated in the data collection, design, analysis, and/or interpretation of the work.

Received: June 5, 2021
Revised: September 15, 2021
Accepted: December 16, 2021
Published: December 21, 2021

REFERENCES

Baden, L.R., El Sahly, H.M., Essink, B., Kotloff, K., Frey, S., Novak, R., Diemert, D., Spector, S.A., Rouphael, N., Creech, C.B., et al. (2021). Efficacy and safety of the mRNA-1273 SARS-CoV-2 vaccine. N. Engl. J. Med. *384*, 403–416.

Bayart, J.-L., Douxfils, J., Gillot, C., David, C., Mullier, F., Elsen, M., Eucher, C., Van Eeckhoudt, S., Roy, T., Gerin, V., et al. (2021). Waning of IgG, total and neutralizing antibodies 6 months post-vaccination with BNT162b2 in healthcare workers. Vaccines (Basel) *9*, 1092.

Campbell, D.J., and Koch, M.A. (2011). Phenotypical and functional specialization of FOXP3+ regulatory T cells. Nat. Rev. Immunol. *11*, 119–130.

Carreño, J.M., Alshammary, H., Singh, G., Raskin, A., Amanat, F., Amoako, A., Gonzalez-Reiche, A.S., van de Guchte, A., Study Group, P., Srivastava, K., et al. (2021). Evidence for retained spike-binding and neutralizing activity against emerging SARS-CoV-2 variants in serum of COVID-19 mRNA vaccine recipients. EBioMedicine *73*, 103626.

Chemaitelly, H., Tang, P., Hasan, M.R., AlMukdad, S., Yassine, H.M., Benslimane, F.M., Al Khatib, H.A., Coyle, P., Ayoub, H.H., Al Kanaani, Z., et al.

(2021). Waning of BNT162b2 vaccine protection against SARS-CoV-2 infection in Qatar. N. Engl. J. Med. *385*, e83.

Ciabattini, A., Pastore, G., Fiorino, F., Polvere, J., Lucchesi, S., Pettini, E., Auddino, S., Rancan, I., Durante, M., Miscia, M., et al. (2021). Evidence of SARS-CoV-2-specific memory B cells six months after vaccination with the BNT162b2 mRNA vaccine. Front. Immunol. *12*, 740708.

Corbett, K.S., Edwards, D.K., Leist, S.R., Abiona, O.M., Boyoglu-Barnum, S., Gillespie, R.A., Himansu, S., Schäfer, A., Ziwawo, C.T., DiPiazza, A.T., et al. (2020). SARS-CoV-2 mRNA vaccine design enabled by prototype pathogen preparedness. Nature *586*, 567–571.

Doria-Rose, N., Suthar, M.S., Makowski, M., O'Connell, S., McDermott, A.B., Flach, B., Ledgerwood, J.E., Mascola, J.R., Graham, B.S., Lin, B.C., et al. (2021). Antibody persistence through 6 months after the second dose of mRNA-1273 vaccine for covid-19. N. Engl. J. Med. *384*, 2259–2261.

Ebinger, J.E., Fert-Bober, J., Printsev, I., Wu, M., Sun, N., Prostko, J.C., Frias, E.C., Stewart, J.L., Van Eyk, J.E., Braun, J.G., et al. (2021). Antibody responses to the BNT162b2 mRNA vaccine in individuals previously infected with SARS-CoV-2. Nat. Med. *27*, 981–984.

Gobbi, F., Buonfrate, D., Moro, L., Rodari, P., Piubelli, C., Caldrer, S., Riccetti, S., Sinigaglia, A., and Barzon, L. (2021). Antibody response to the bnt162b2 mrna covid-19 vaccine in subjects with prior sars-cov-2 infection. Viruses *13*, 422.

Goel, R.R., Apostolidis, S.A., Painter, M.M., Mathew, D., Pattekar, A., Kuthuru, O., Gouma, S., Hicks, P., Meng, W., Rosenfeld, A.M., et al. (2021). Distinct antibody and memory B cell responses in SARS-CoV-2 naïve and recovered individuals following mRNA vaccination. Sci. Immunol. *6*, eabi6950.

Goldberg, Y., Mandel, M., Bar-On, Y.M., Bodenheimer, O., Freedman, L., Haas, E.J., Milo, R., Alroy-Preis, S., Ash, N., and Huppert, A. (2021). Waning immunity after the BNT162b2 vaccine in Israel. N. Engl. J. Med. *385*, e85.

Grifoni, A., Weiskopf, D., Ramirez, S.I., Mateus, J., Dan, J.M., Moderbacher, C.R., Rawlings, S.A., Sutherland, A., Premkumar, L., Jadi, R.S., et al. (2020). Targets of T Cell responses to SARS-CoV-2 coronavirus in humans with COVID-19 disease and unexposed individuals. Cell *181*, 1489–1501.e15.

Guerrera, G., Picozza, M., D'Orso, S., Placido, R., Pirronello, M., Verdiani, A., Termine, A., Fabrizio, C., Giannessi, F., Sambucci, M., et al. (2021). BNT162b2 vaccination induces durable SARS-CoV-2 specific T cells with a stem cell memory phenotype. Sci. Immunol. *6*, eabl5344.

Kadire, S.R., Wachter, R.M., and Lurie, N. (2021). Delayed second dose versus standard regimen for covid-19 vaccination. N. Engl. J. Med. *384*, e28.

Krammer, F., Srivastava, K., Alshammary, H., Amoako, A.A., Awawda, M.H., Beach, K.F., Bermúdez-González, M.C., Bielak, D.A., Carreño, J.M., Chernet, R.L., et al. (2021). Antibody responses in seropositive persons after a single dose of SARS-CoV-2 mRNA vaccine. N. Engl. J. Med. *384*, 1372–1374.

Levi, R., Azzolini, E., Pozzi, C., Ubaldi, L., Lagioia, M., Mantovani, A., and Rescigno, M. (2021). One dose of SARS-CoV-2 vaccine exponentially increases antibodies in individuals who have recovered from symptomatic COVID-19. J. Clin. Invest. *131*, e149154.

Mahase, E. (2021). Covid-19: third vaccine dose boosts immune response but may not be needed, say researchers. BMJ *373*, n1659.

McInnes, L., Healy, J., and Melville, J. (2020). UMAP: uniform manifold approximation and projection for dimension reduction. ArXiv, 1802.03426.

McMahan, K., Yu, J., Mercado, N.B., Loos, C., Tostanoski, L.H., Chandrashekar, A., Liu, J., Peter, L., Atyeo, C., Zhu, A., et al. (2021). Correlates of protection against SARS-CoV-2 in rhesus macaques. Nature *590*, 630–634.

Mulligan, M.J., Lyke, K.E., Kitchin, N., Absalon, J., Gurtman, A., Lockhart, S., Neuzil, K., Raabe, V., Bailey, R., Swanson, K.A., et al. (2020). Phase I/II study of COVID-19 RNA vaccine BNT162b1 in adults. Nature *586*, 589–593.

Naaber, P., Tserel, L., Kangro, K., Sepp, E., Jürjenson, V., Adamson, A., Haljasmägi, L., Rumm, A.P., Maruste, R., Kärner, J., et al. (2021). Dynamics of antibody response to BNT162b2 vaccine after six months: a longitudinal prospective study. Lancet Reg. Health Eur. *10*, 100208.

Ni, L., Ye, F., Cheng, M.L., Feng, Y., Deng, Y.Q., Zhao, H., Wei, P., Ge, J., Gou, M., Li, X., et al. (2020). Detection of SARS-CoV-2-specific humoral and cellular immunity in COVID-19 convalescent individuals. Immunity *52*, 971–977.e3.

Noori, M., Nejadghaderi, S.A., Arshi, S., Carson-Chahhoud, K., Ansarin, K., Kolahi, A.-A., and Safiri, S. (2021). Potency of BNT162b2 and mRNA-1273 vaccine-induced neutralizing antibodies against severe acute respiratory syndrome-CoV-2 variants of concern: a systematic review of in vitro studies. Rev. Med. Virol., e2277.

Polack, F.P., Thomas, S.J., Kitchin, N., Absalon, J., Gurtman, A., Lockhart, S., Perez, J.L., Pérez Marc, G., Moreira, E.D., Zerbini, C., et al. (2020). Safety and efficacy of the BNT162b2 mRNA covid-19 vaccine. N. Engl. J. Med. *383*, 2603–2615.

Prendecki, M., Clarke, C., Brown, J., Cox, A., Gleeson, S., Guckian, M., Randell, P., Pria, A.D., Lightstone, L., Xu, X.N., et al. (2021a). Effect of previous SARS-CoV-2 infection on humoral and T-cell responses to single-dose BNT162b2 vaccine. Lancet *397*, 1178–1181.

Prendecki, M., Clarke, C., Brown, J., Cox, A., Gleeson, S., Guckian, M., Randell, P., Pria, A.D., Lightstone, L., Xu, X.-N., et al. (2021b). Effect of previous SARS-CoV-2 infection on humoral and T-cell responses to single-dose BNT162b2 vaccine. Lancet *397*, 1178–1181.

Sasikala, M., Shashidhar, J., Deepika, G., Ravikanth, V., Krishna, V.V., Sadhana, Y., Pragathi, K., and Reddy, D.N. (2021). Immunological memory and neutralizing activity to a single dose of COVID-19 vaccine in previously infected individuals. Int. J. Infect. Dis. *108*, 183–186.

Sattler, A., Angermair, S., Stockmann, H., Heim, K.M., Khadzhynov, D., Treskatsch, S., Halleck, F., Kreis, M.E., and Kotsch, K. (2020). SARS–CoV-2–specific T cell responses and correlations with COVID-19 patient predisposition. J. Clin. Invest. *130*, 6477–6489.

Sokal, A., Chappert, P., Barba-Spaeth, G., Roeser, A., Fourati, S., Azzaoui, I., Vandenberghe, A., Fernandez, I., Meola, A., Bouvier-Alias, M., et al. (2021). Maturation and persistence of the anti-SARS-CoV-2 memory B cell response. Cell *184*, 1201–1213.e14.

Thomas, S.J., Moreira, E.D., Kitchin, N., Absalon, J., Gurtman, A., Lockhart, S., Perez, J.L., Pérez Marc, G., Polack, F.P., Zerbini, C., et al. (2021). Safety and efficacy of the BNT162b2 mRNA covid-19 vaccine through 6 months. N. Engl. J. Med. *385*, 1761–1773.

Turner, J.S., O'Halloran, J.A., Kalaidina, E., Kim, W., Schmitz, A.J., Zhou, J.Q., Lei, T., Thapa, M., Chen, R.E., Case, J.B., et al. (2021). SARS-CoV-2 mRNA vaccines induce persistent human germinal centre responses. Nature *596*, 109–113.

Voysey, M., Clemens, S.A.C., Madhi, S.A., Weckx, L.Y., Folegatti, P.M., Aley, P.K., Angus, B., Baillie, V.L., Barnabas, S.L., Bhorat, Q.E., et al. (2021). Safety and efficacy of the ChAdOx1 nCoV-19 vaccine (AZD1222) against SARS-CoV-2: an interim analysis of four randomised controlled trials in Brazil, South Africa, and the UK. Lancet *397*, 99–111.

Walsh, E.E., Frenck, R.W., Falsey, A.R., Kitchin, N., Absalon, J., Gurtman, A., Lockhart, S., Neuzil, K., Mulligan, M.J., Bailey, R., et al. (2020). Safety and immunogenicity of two RNA-based covid-19 vaccine candidates. N. Engl. J. Med. *383*, 2439–2450.

STAR★METHODS

KEY RESOURCES TABLE

REAGENT or RESOURCE	SOURCE	IDENTIFIER
Antibodies		
Anti-human CD45RA BUV395 (clone 5H9)	BD	Cat# 740315; RRID:AB_2740052
Anti-human CD16 BUV496 (clone 3G8)	BD	Cat# 612944; RRID:AB_2870224
Anti-human CCR5 BUV563 (clone 3A9)	BD	Cat# 741401; RRID:AB_2870893
Anti-human CD62L BUV615 (clone SK11)	BD	Cat# 751364; RRID:AB_2875371
Anti-CD11c BUV661 (clone B-Ly6)	BD	Cat# 612967; RRID:AB_2870241
Anti-human CCR7 BUB737 (clone 2-L1-A)	BD	Cat# 749676; RRID:AB_2873937
Anti-human CD56 BUB737 (clone NCAM 16.2)	BD	Cat# 612766; RRID:AB_2813880
Anti-human CD8 BUV805 (clone SK1)	BD	Cat# 612889; RRID:AB_2833078
Anti-human IgD BV480 (clone IA6-2)	BD	Cat# 566138; RRID:AB_2739536
Anti-human IgG BV605 (clone G18-145)	BD	Cat# 563246; RRID:AB_2738092
Anti-human CXCR5 BV750 (clone RF8B2)	BD	Cat# 747111; RRID:AB_2871862
Anti-human CD141 BB515 (clone 1A4)	BD	Cat# 566017; RRID:AB_2739462
Anti-human CD127 APC/R700 (clone HIL-7R-M21)	BD	Cat# 565185; RRID:AB_2739099
Anti-human IL-2 APC/R700 (clone MQ1-17H12)	BD	Cat# 565136; RRID:AB_2739079
Anti-human CD163 BB790 (clone GHI/61)	BD	Cat# 624296; RRID:AB_2214940
Anti-human NKG2C BB700 (clone 134519)	BD	Cat# 748162; RRID: AB_2872623
Anti-human CD123 SuperBright436 (clone 6H6)	ThermoFisher Scientific	Cat# 62-1239-42; RRID:AB_2662727
Anti-human CD161 eFluor 450 (clone HP-3G10)	ThermoFisher Scientific	Cat# 48-1619-42; RRID:AB_10854273
Anti-human CD8 Pacific Orange (clone 3B5)	ThermoFisher Scientific	Cat# MHCD0830; RRID:AB_10372066
Anti-human CD20 Pacific Orange (clone 2H7)	ThermoFisher Scientific	Cat# MHCD2030; RRID:AB_10375578
Anti-human TCRγδ PerCP-eFluor 710 (clone B1.1)	ThermoFisher Scientific	Cat# 46-9959-42; RRID:AB_2573926
Anti-human CD25 PE-AlexaFluor700 (clone CD25-3G10)	ThermoFisher Scientific	Cat# MHCD2524; RRID:AB_2539740
Anti-human CCR7 BV421 (clone G043H7)	Biolegend	Cat# 353208; RRID:AB_11203894
Anti-human CD3 BV510 (clone OKT3)	Biolegend	Cat# 317332; RRID:AB_2561943
Anti-human CD3 BV570 (clone UCHT1)	Biolegend	Cat# 300436; RRID:AB_2562124
Anti-human CD4 BV570 (clone RPA-T4)	Biolegend	Cat# 300534; RRID:AB_2563791
Anti-human CD4 cFluor-YG584 (clone K3)	Cytek Biosciences	Cat# R7-20042; RRID: AB_2885083
Anti-human IgM BV570 (clone MHM-88)	Biolegend	Cat# 314517; RRID:AB_10913816
Anti-human CD28 BV650 (clone CD28.2)	Biolegend	Cat# 302946; RRID:AB_2616855
Anti-human TNFα BV650 (clone MAb11)	BD	Cat# 563418; RRID:AB_2738194
Anti-human CCR6 BV711 (clone G034E3)	Biolegend	Cat# 353436; RRID:AB_2629608
Anti-human IFNγ BV711 (clone 4S.B3)	Biolegend	Cat# 502540; RRID:AB_2563506)
Anti-human PD-1 BV785 (clone EH12.2H7)	Biolegend	Cat# 329929; RRID:AB_11218984
Anti-human CD57 FITC (clone HNK-1)	Biolegend	Cat# 359604; RRID:AB_2562387
Anti-human CD3 SparkBlue550 (clone SK7)	Biolegend	Cat# 344852; RRID:AB_2819985

(*Continued on next page*)

Continued

REAGENT or RESOURCE	SOURCE	IDENTIFIER
Anti-human CD14 SparkBlue550 (clone 63D3)	Biolegend	Cat# 367148; RRID:AB_2832724
Anti-human CD45 PerCP (clone 2D1)	Biolegend	Cat# 368506; RRID:AB_2566358
Anti-human CD4 PerCP/Cy5.5 (clone SK3)	Biolegend	Cat# 344608; RRID:AB_1953236
Anti-human CD11b PerCP/Cy5.5 (clone ICRF44)	Biolegend	Cat# 301328; RRID:AB_10933428
Anti-human PD-L1 PE (clone 10F.9G2)	Biolegend	Cat# 124308; RRID:AB_2073556
Anti-human CD24 PE/Dazzle594 (clone ML5)	Biolegend	Cat# 311134; RRID:AB_2566349
Anti-human CD95 PE/Cy5 (clone DX2)	Biolegend	Cat# 305610; RRID:AB_314548
Anti-human CXCR3 PE/Cy7 (clone G025H7)	Biolegend	Cat# 353720; RRID:AB_11219383
Anti-human Granzyme B PE/Cy7 (clone QA16A02)	Biolegend	Cat# 372214; RRID:AB_2728381
Anti-human CD27 APC (clone M-T271)	Biolegend	Cat# 356410; RRID:AB_2561957
Anti-human CD1c AlexaFluor647 (clone L161)	Biolegend	Cat# 331510; RRID:AB_1186032
Anti-human CD19 SparkNIR685 (clone HIB19)	Biolegend	Cat# 302270; RRID:AB_2832581
Anti-human HLA-DR APC/Fire750 (clone L243)	Biolegend	Cat# 307658; RRID:AB_2572101
Anti-human CD38 APC/Fire810 (clone HIT2)	Biolegend	Cat# 303550; RRID:AB_2860784
Biological samples		
Blood samples of Healthy Health Personnel	This paper	N/A
Chemicals, peptides, and recombinant proteins		
Ficoll-Plus	GE Healthcare	Cat# 17-1440-03
RPMI 1640 Medium	Thermo Fisher Scientific	Cat# 11594506
DMEM Medium	Thermo Fisher Scientific	Cat# 11965092
Phosphate buffer saline (PBS)	Sigma	Cat# P4417-100TAB
Bovine serum albumin (BSA)	Sigma	Cat# A9647-1KG
Foetal Bovine Serum (FBS)	Thermo Fisher Scientific	Cat# 11560636
Carboxyfluorescein succinimidyl ester (CFSE)	Thermo Fisher Scientific	Cat# C34554
PepTivator SARS-CoV-2 Prot_S	Miltenyi Biotec	Cat# 130-126-701
Protein Transport Inhibitor (Containing Brefeldin A)	BD	Cat# 555029
Protein Transport Inhibitor (Containing Monensin)	BD	Cat# 554724
LIVE/DEAD Fixable Blue Dead Cell Stain Kit	Thermo Fisher Scientific	Cat# L34962
True –Stain Monocyte Blocker	Biolegend	Cat# 426103
Brilliant Stain Buffer	BD	Cat# 566349
Dimethyl sulfoxide (DMSO)	Sigma	Cat# 67-68-5
Critical commercial assays		
Cytofix/Cytoperm Fixation/ Permeabilization Kit	BD	Cat# 554714
COVID-19 (SARS-CoV-2) quantitative IgG ELISA	Demeditec	Cat# DECOV1901Q
LEGENDplex SARS-CoV-2 Serological IgA Panel (2-plex)	Biolegend	Cat# 741139
LEGENDplex SARS-CoV-2 Serological IgG Panel (3-plex)	Biolegend	Cat# 741131

(*Continued on next page*)

Continued

REAGENT or RESOURCE	SOURCE	IDENTIFIER
LEGENDplex SARS-CoV-2 Neut. Ab Assay (1-plex)	Biolegend	Cat# 741126
LEGENDplex HU Essential Immune Response Panel (13-plex)	Biolegend	Cat# 740930
SARS-CoV-2 Spike B Cell Analysis Kit, human	Miltenyi Biotec	Cat# 130-128-022
Experimental models: Cell lines		
Vero E6	ATCC	Cat# CRL-1586, RRID:CVCL_0574
Recombinant DNA		
pNL4–3ΔenvRen	This paper	N/A
pcDNA3.1-SCoV2Δ19-D614	This paper	N/A
p24Gag	This paper	N/A
Software and algorithms		
LEGENDplex software v.8	Biolegend	https://www.biolegend.com/en-us/legendplex
Prism version 8.3	GraphPad	https://www.graphpad.com/scientific-software/prism/
FlowJo v.10.6.2	TreeStar	https://www.flowjo.com/

RESOURCE AVAILABILITY

Lead contact

Further information and requests for resources and reagents should be directed to and will be fulfilled by the Lead Contact Eduardo López-Collazo (elopezc@salud.madrid.es).

Material availability

This study did not generate new unique reagents.

Data and code availability

- Data reported in this paper will be shared by the lead contact upon request.
- This paper does not report original code.
- Any additional information required to reanalyze the data reported in this paper is available from the lead contact upon request.

EXPERIMENTAL MODEL AND SUBJECT DETAILS

Healthy health personnel volunteers and longitudinal samples

A total of 27 healthy health personnel volunteers of the Research Institution of La Paz University Hospital of Madrid (Spain) were enrolled for this study before vaccination against Spike protein of SARS-CoV-2 (BNT162b2 SARS-CoV-2 mRNA vaccine of Pfizer & BioNTech). Blood samples were taken at four times: 5 days before the vaccination (sample 0), 14 days after the first dose of vaccine (sample 1), 14 days after the second dose of vaccine (sample 2) and 230 days after the second dose (sample 3) (Figure 1A). Informed consent was obtained from all volunteers in accordance with the ethical standards and following the ethical guidelines of the 1975 Declaration of Helsinki. All healthy health personnel data were anonymized before study inclusion and their details are summarized in Table S1.

Culture conditions of primary and Vero E6 cells

Fresh and thawed Peripheral Blood Mononuclear Cells (PBMCs) were cultured in RPMI 1640 medium containing 10% fetal bovine serum (FBS), 25 mM HEPES, 2 mM L-glutamine and 1% Penicillin and Streptomycin Mix (Gibco) before some stimulation to their activation or proliferation. PBMCs were cultured at 37 °C at 5% CO_2 in a humidified incubator. Vero E6 were cultured in in DMEM containing 10% fetal bovine serum (FBS), 2 mM L-glutamine and 1% Penicillin and Streptomycin Mix (Gibco).

METHOD DETAILS

PBMCs isolation, storage and thawing procedure

Peripheral blood mononuclear cells (PBMCs) from healthy health personnel vaccinated with BNT162b2 SARS-CoV-2 mRNA vaccine were isolated from EDTA anticoagulant venous blood using Ficoll-Plus (GE Healthcare Bio-Sciences) solution according to the manufacturer's instructions. PBMCs were washed twice with phosphate buffer saline (PBS) and counted using Trypan blue staining. A part of cells was resuspended in two aliquots of 6×10^6 cells in fetal bovine serum (FBS) containing 10% DMSO (Sigma-Aldrich). Then, aliquoted PBMCs were slowly frozen ($-1°C$/minute) using a controlled-grade freezing device (Mr. Frosty, ThermoFisher Scientific) and stored for 24 hours at -80 ºC before storage in liquid nitrogen. For use PBMCs, they were rapidly thawed in a water bath at 37°C and washed twice with RPMI 1640 medium containing 10% fetal bovine serum (FBS), 25 mM HEPES, 2 mM L-glutamine and 1% Penicillin and Streptomycin Mix (PenStrep, Gibco).

Plasma collection

Plasma samples from healthy health personnel vaccinated with the Pfizer vaccine against SARS-CoV-2 were obtained from EDTA anticoagulant venous blood using Ficoll-Plus (GE Healthcare Bio-Sciences) solution according to standard density gradient centrifugation method. Then, they were aliquoted and stored at $-80°C$ until use.

Algorithm for dimensionality reduction

Uniform Manifold Approximation and Projection (UMAP) analysis was carried out using all markers listed in Table S2. Data were manually gated to remove aggregates, dead cells, debris, and CD45 negative events, and then they were sub-sampled to include 60% of $CD45^+$ live singlets from each sample. Subsequently, the UMAP analysis was performed to visualize the different subpopulations in groups. $CD3^+$ and $CD19^+$ subpopulations were defined as $CD3^+/TCR\gamma\delta^-/CD56^-/CD14^-/CD4^+$ or $CD8^+$, and $CD3^-/TCR\gamma\delta^-/CD56^-/CD14^-/CD19^+/CD20^{+/}$, respectively, prior to the UMAP analysis. UMAP settings for $CD3^+$ subpopulation used CD45RA, CD28, CCR7, PD-1, CD27, CD57, CD127, CD25, CD95, CD38 and HLA-DR fluorescent parameters. UMAP settings for $CD19^+$ subpopulation used CD38, CD27, CD19, CD24, IgD, IgM, IgG and CD20 fluorescent parameters. All fluorescent parameters were used besides lived and $CD45^+$ cells. UMAP was run using 15 nearest neighbors, a minimal distance of 0.5, in 2-dimensions and Euclidean distance and spectral initialization mode (McInnes et al., 2020). Data were analyzed using FlowJo (TreeStar) v10.6.2 software.

Detection of anti-spike IgA and IgG SARS-CoV-2 antibodies

For detection of specific antibodies IgA and IgG against the Spike protein of SARS-CoV-2, reserved plasma samples from healthy health personnel vaccinated with the Pfizer vaccine against SARS-CoV-2 stored at $-80°C$ were thawed and centrifuged at 1000 relative centrifugal force for 30 minutes to remove particulates prior to use. The title of IgA antibodies in plasma samples were performed by the bead-based multiplex assay, LEGENDplex SARS-CoV-2 Serological IgA Panel (2-plex, Spike (S1) and receptor binding domain (RBD) of Spike protein) (Biolegend) according to the manufacturer's instructions. The title of IgG antibodies in plasma samples were performed by the bead-based multiplex assay, LEGENDplex SARS-CoV-2 Serological IgG Panel (3-plex, Spike (S1), receptor binding domain (RBD) of Spike protein and nucleocapsid (N)) (Biolegend) according to the manufacturer's instructions. Samples were acquired on a FACSCalibur flow cytometer (BD Biosciences) and data were analyzed using LEGENDplex (Biolegend) v.8 software. For quantification of IgG antibodies against full Spike protein of SARS-CoV-2, COVID-19 quantitative IgG ELISA kit from Demeditec Diagnostics GmbH (Ref.: DECOV1901Q) was used. Data obtained were corroborated by Eurofins-Ingenasa kits: INGEZIM®-NP-COVID 19 DR and INGEZIM®-RBD-COVID 19 DR.

Detection of neutralization capacity of plasma against SARS-CoV-2 Spike antigen

The neutralizing antibodies in plasma samples were performed by a competitive immunoassay of ACE2-conjugated beads, LEGENDplex SARS-CoV-2 Neut. Ab Assay (1-plex) according to the manufacturer's instructions.

To measure neutralising antibodies titres by means of viral pseudoparticles, diluted plasma samples were preincubated with pseudoviruses generated by co-transfection of the plasmid pNL4–3ΔenvRen and an expression vector for the viral SARS-CoV-2 Spike (pcDNA3.1-SCoV2Δ19-D614) and added at a concentration of 10 ng p24Gag per well to Vero E6 cells in 96-well plates. At 48 h post infection, viral infectivity was assessed by measuring luciferase activity (Renilla Luciferase Assay (Promega, Madison, WI, USA) using a 96-well plate luminometer LB 960 Centro XS (Berthold Technologies, Oak Ridge, TN, USA). The titre of neutralising antibodies was calculated as 50% inhibitory dose (neutralising titre 50, NT50), expressed as reciprocal of four-fold serial dilution of heat-inactivated sera (range 1:32–1:8192), resulting in a 50% reduction of pseudovirus infection compared with control without serum. Samples below the detection threshold (1:32 serum dilution) were given 1:16 value. Positive and negative controls were included in the assay and non-specific neutralisation was assessed using a nonrelated pseudovirus expressing the vesicular stomatitis virus envelope.

Antibodies and immunophenotyping by flow cytometry

Stored PBMCs were thawed as we have described above and they were rested in RPMI 1640 medium containing 10% fetal bovine serum (FBS), 25 mM HEPES, 2 mM L-glutamine and 1% Penicillin and Streptomycin Mix (Gibco) for 1 hour previous the staining

protocol. Then, PBMCs were stained with fluorochrome-conjugated antibodies to a multi-colour panel of surface markers listed in Table S2. Dead cells were excluded using LIVE/DEAD Blue fluorescent reactive dye purchased from Invitrogen and True-Stain Monocyte Blocker (BioLegend) reagent was added prior to the label protocol to block the nonspecific binding of some fluorochromes on monocytes. Labeled cells were acquired on a Cytek Aurora Spectral Cytometer (Cytek Biosciences). Data were analyzed using FlowJo (TreeStar) v10.6.2 software.

SARS-CoV-2 Spike-specific B cells detection

SARS-CoV-2 Spike-specific B cells were detected in sample 3 by means of the SARS-CoV-2 Spike B cell analysis kit provided by Miltenyi Biotec, following the manufacturer's instructions. Labeled cells were acquired on a Cytek Aurora Spectral Cytometer (Cytek Biosciences). Data were analyzed using FlowJo (TreeStar) v10.6.2 software.

SARS-CoV-2 Spike-specific T cell proliferation assays and supernatant collection

Fresh PBMCs from healthy health personnel 14 (sample 2) and 230 (sample 3) days after the second dose of BNT162b2 SARS-CoV-2 mRNA vaccine isolated from EDTA anticoagulant venous blood using Ficoll-Plus (GE Healthcare Bio-Sciences) were washed twice with phosphate buffer saline (PBS) and counted using Trypan blue staining. Carboxyfluorescein succinimidyl ester (CFSE) was purchased from Thermo Fisher Scientific and used following the manufacturer's protocol to assess T lymphocyte proliferation. After that, living CFSE-labeled PBMCs were plated in RPMI 1640 medium containing 10% fetal bovine serum (FBS), 25 mM HEPES, 2 mM L-glutamine and 1% Penicillin and Streptomycin Mix (Gibco) in a 96-wells plate flat bottom ($1,5 \times 10^6$ cells/well) and stimulated or not with Peptivator SARS-CoV-2 Prot_S (Miltenyi Biotec) for 5 days at 37°C at 5% CO_2. After proliferation assay, supernatants were collected, aliquoted and stored at −80°C until use. Then, PBMCs were washed and stained with fluorochrome-conjugated antibodies to surface markers listed in Table S3.

Supernatant soluble cytokine quantification

Reserved and stored supernatants of PBMCs from healthy health personnel 14 (sample 2) and 230 (sample 3) days after the second dose of BNT162b2 SARS-CoV-2 mRNA vaccine, stimulated with Peptivator SARS-CoV-2 Prot_S (Miltenyi Biotec) for 5 days, were thawed. The concentration measurements of cytokines in supernatant samples was performed by the bead-based multiplex assay, LEGENDplex Human Essential Immune Response Panel (13-plex: IL-1β, IL-2, IL-4, IFN-γ, TNF-α, MCP-1 (CCL2), CXCL10, IL-6, IL-8 (CXCL8), IL-10, IL-12p70, IL-17A and Free Active TGF-β1), according to the manufacturer's instructions. Samples were acquired on a FACSCalibur flow cytometer (BD Biosciences) and data were analyzed using LEGENDplex (BioLegend) v.8 software.

PBMCs stimulation and intracellular cytokine staining

Thawed PBMCs were stimulated with Peptivator SARS-CoV-2 Prot_S (Miltenyi Biotec) consisting in a pool of 15-mer sequences with 11 amino acids overlap covering the immunodominant sequence domains of the Spike glycoprotein of SARS-CoV-2. Incubation was performed for 6 hours at 37°C 5% CO_2 in presence of Golgi-Plug containing Brefeldin A (BD) and Golgi-Stop containing Monensin (BD) added after 1 hour of the stimulation according to the manufacturer's instructions. After that, PBMCs were washed and stained with the surface markers (listed in Table S4) for 30 minutes at room temperature, twice washed, fixed and permeabilized using the Cytofix/Cytoperm Fixation/Permeabilization Kit (BD) according the manufacturer's instructions. Subsequently, the fixed and permeabilized PBMCs were staining using fluorochrome-conjugated antibodies against intracellular makers listed in Table S4. Labeled cells were acquired on a Cytek Aurora Spectral Cytometer (Cytek Biosciences). Data were analyzed using FlowJo (TreeStar) v10.6.2 software.

QUANTIFICATION AND STATISTICAL ANALYSIS

Statistical analysis of biological data

Data are expressed as violin and box plots with mean and interquartile ranges, mean ± SEM, and single dots representing an individual subject each. D'Agostino & Pearson Normality test was performed to all the studied variables. Student's t-test for two groups comparison of quantitative variables, either unpaired (t-test or Mann-Whitney) or paired (t-test or Wilcoxon), and ANOVA or Kruskal-Wallis for multiple groups comparisons of quantitative variables were performed. Correlation between quantitative variables were evaluated by Spearman's analysis. All along figures, p-values (P) are denoted as ns: non-significant, *$P < 0.05$, **$P < 0.01$, ***$P < 0.001$, ****$P < 0.0001$.

In order to perform a visual correlation analysis between the expression of different immune factors, and COVID-19 history of the subjects, the raw data of each one was normalized using the Z-Score strategy ((value-μ)/σ). The hierarchical clustering analysis was developed by heatmap, geom tile and ggplot2 packages (version 1.16.0) in R language (version 4.0.2). This package is available at https://www.r-graph-gallery.com/heatmap. The clustering was analyzed and distributed by average linkage method, in which the distance between two clusters is defined as the mean of distances between all pairs of objects, where each pair is made up of one object from each group. Measurement method between rows and columns was performed by Manhattan method.

Cell Reports, Volume *38*

Supplemental information

Cellular and humoral functional responses after BNT162b2 mRNA vaccination differ longitudinally between naive and subjects recovered from COVID-19

Roberto Lozano-Rodríguez, Jaime Valentín-Quiroga, José Avendaño-Ortiz, Alejandro Martín-Quirós, Alejandro Pascual-Iglesias, Verónica Terrón-Arcos, Karla Montalbán-Hernández, José Carlos Casalvilla-Dueñas, Marta Bergón-Gutiérrez, José Alcamí, Javier García-Pérez, Almudena Cascajero, Miguel Ángel García-Garrido, Álvaro del Balzo-Castillo, María Peinado, Laura Gómez, Irene Llorente-Fernández, Gema Martín-Miguel, Carmen Herrero-Benito, José Miguel Benito, Norma Rallón, Carmen Vela-Olmo, Lissette López-Morejón, Carolina Cubillos-Zapata, Luis A. Aguirre, Carlos del Fresno, and Eduardo López-Collazo

SUPPLEMENTAL INFORMATION

Cellular and humoral functional responses after BNT162b2 mRNA vaccination differ longitudinally between naïve and COVID-19-recovered individuals

Roberto Lozano-Rodríguez, Jaime Valentín-Quiroga, José Avendaño-Ortiz, Alejandro Martín-Quirós, Alejandro Pascual-Iglesias, Verónica Terrón, Karla Montalbán-Hernández, José Carlos Casalvilla-Dueñas, Marta Bergón-Gutierrez, José Alcamí, Javier García-Pérez, Almudena Cascajero, Miguel Ángel García-Garrido, Álvaro del Balzo-Castillo, María Peinado, Laura Gómez, Irene Llorente-Fernández, Gema Martín-Miguel, Carmen Herrero-Benito, José Miguel Benito, Norma Rallón, Carmen Vela-Olmo, Lissette López-Morejón, Carolina Cubillos-Zapata, Luis A. Aguirre, Carlos del Fresno and Eduardo López-Collazo

SUPPLEMENTARY FIGURES

Supplementary Figure 1

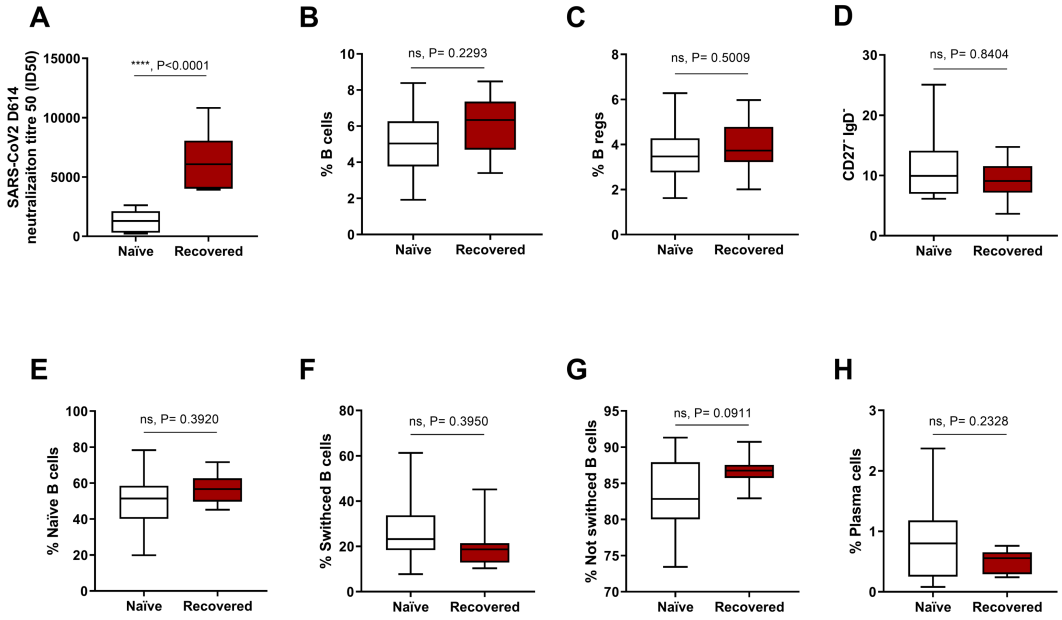

Figure S1. Neutralizing capacity and B cell subpopulation frequencies after vaccination in naïve and COVID-19-recovered individuals in sample 2. (**A**) Functional neutralizing antibody titles on plasma of naïve and COVID-19-recovered individuals against Spike expressing-pseudovirus. Results are expressed as the dilution of sera that inhibited infection by 50% (NT50). (**B**) Frequency of B cells ($CD19^+CD20^+$) gated on live leucocytes ($CD45^+$) in naïve and COVID-19-recovered individuals. Frequency of $CD24^+CD38^+$ B regs (**C**), $CD27^+IgD^-$ B cells (**D**), naïve $CD27^-IgD^+$ B cells (**E**), switched $CD27^+IgD^-$ B cells (**F**), not switched $CD27^+IgD^+$ B cells (**G**) and $CD38^+CD27^+$ plasma cells (**H**) gated on $CD19^+CD20^+$ B cells in naïve and COVID-19-recovered individuals. (A-H) Data shown as mean ± SEM. (A-H) Unpaired Student's t-test (ns, not significant; ****, P<0.0001).

Supplementary Figure 2

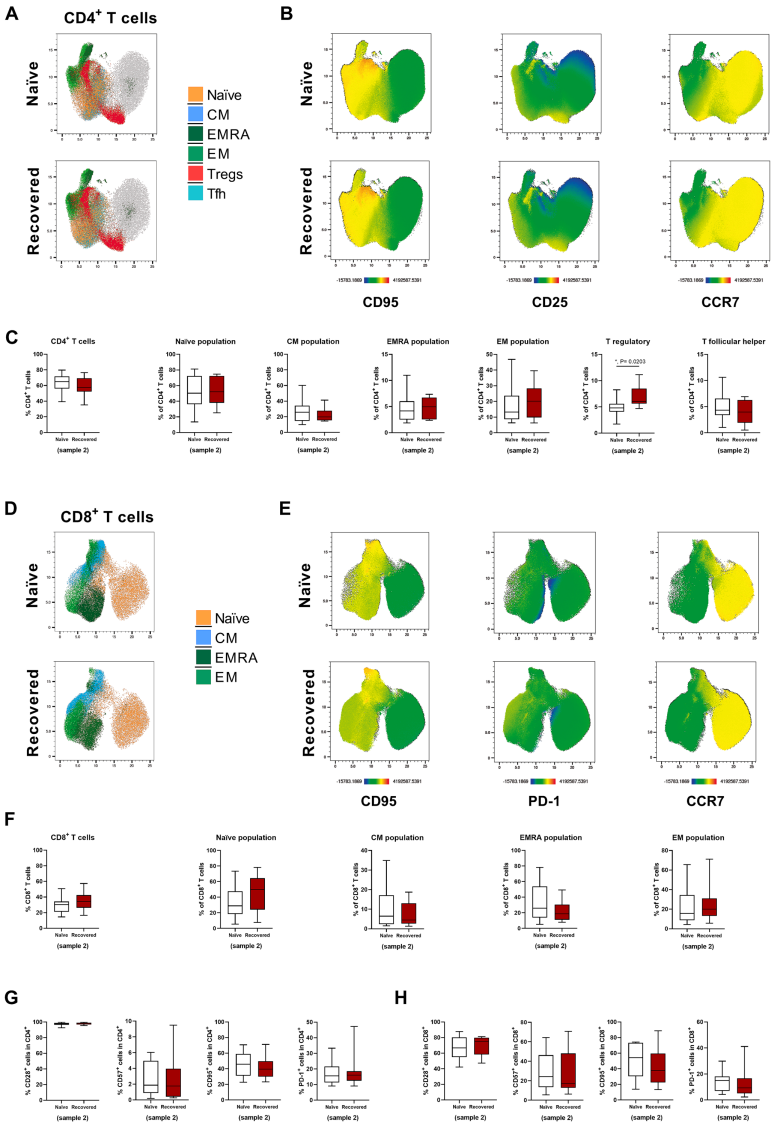

Figure S2. T cell phenotype and subpopulation frequencies after vaccination in naïve and COVID-19-recovered individuals in sample 2. (**A**) Uniform Manifold Approximation and Projection (UMAP) of $CD4^+$ T cells from naïve and COVID-19-recovered individuals followed by manual gating to identify naïve ($CD45RA^+CCR7^+$), central memory (CM) ($CD45RA^-CCR7^+$), effector memory cells re-expressing CD45RA (EMRA) ($CD45RA^+CCR7^-$), effector memory (EM) ($CD45RA^-CCR7^-$), regulatory (Tregs) ($CD25^+CD127^-$) and follicular helper (Tfh) ($CXCR5^+CD45RA^-$) T cells. (**B**) UMAP clustering expressions of CD95, CD25 and CCR7 on $CD4^+$ T cells from naïve and COVID-19-recovered individuals. (**C**) Frequency of total and different $CD4^+$ T cell subsets in naïve and COVID-19-recovered individuals. (**D**) UMAP of $CD8^+$ T cells from naïve and COVID-19-recovered individuals followed by manual gating to identify naïve ($CD45RA^+CCR7^+$), central memory (CM) ($CD45RA^-CCR7^+$), effector memory cells re-expressing CD45RA (EMRA) ($CD45RA^+CCR7^-$) and effector memory (EM) ($CD45RA^-CCR7^-$). (**E**) UMAP clustering expressions of CD95, CD25 and CCR7 on $CD8^+$ T cells from naïve and COVID-19-recovered individuals. (**F**) Frequency of total and different $CD8^+$ T cell subsets in naïve and COVID-19-recovered individuals. Expression levels of CD28, CD57, CD95 and PD-1 in $CD4^+$ (**G**) and $CD8^+$ (**H**) T cells from naïve and COVID-19-recovered individuals. (C, F-H) Data shown as mean ± SEM. (C, F-H) Unpaired Student's t-test (*, $P<0.05$).

Supplementary Figure 3

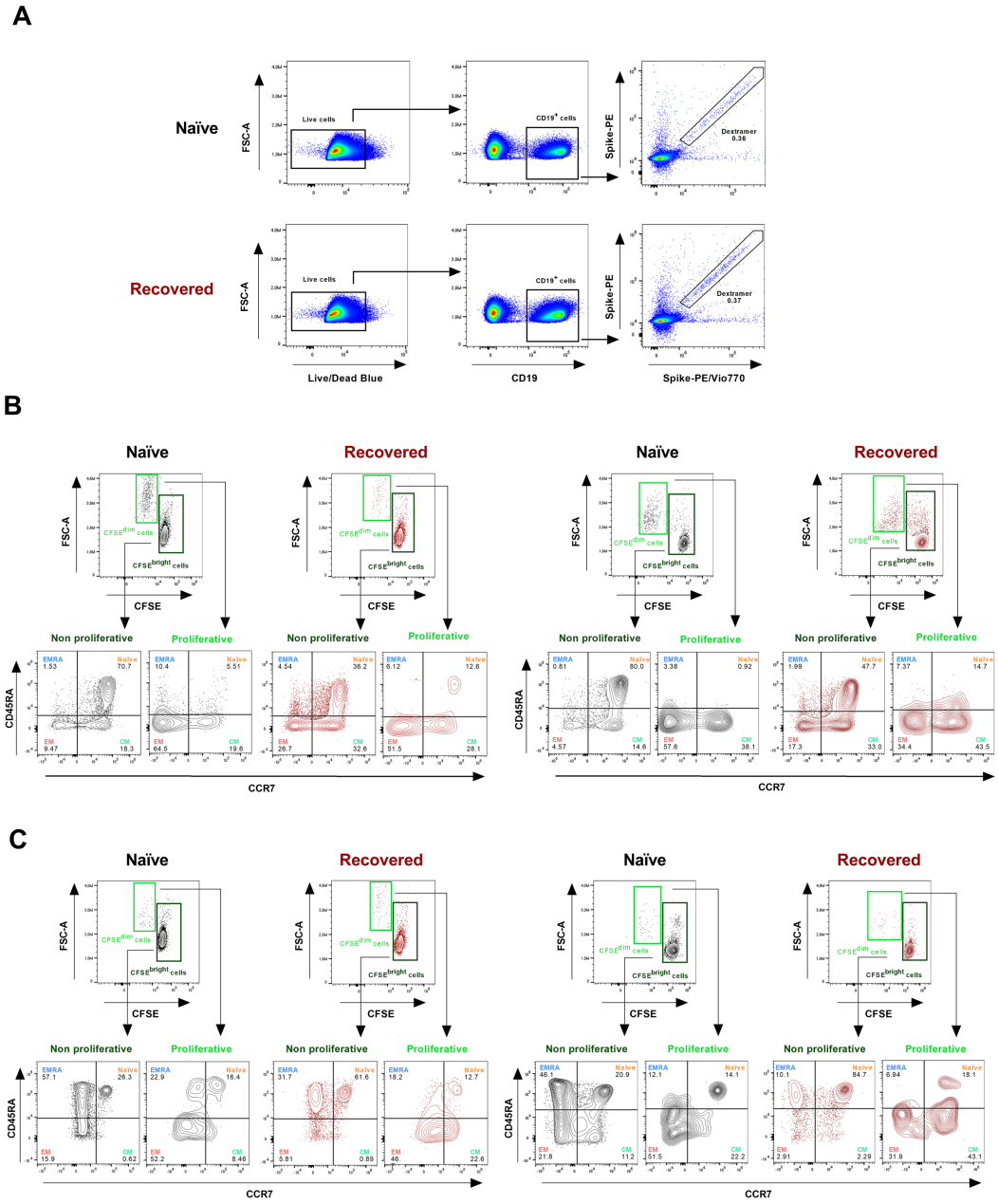

Figure S3. Gating strategies. (**A**) Representative gating to identify SARS-CoV-2 S-protein-specific B cells ($CD19^{+}$) in PBMCs from sample 3 (230 days after the second dose of the BNT162b2 vaccine). PBMCs were labelled with CFSE and stimulated with SARS-CoV-2 spike peptide pool for 5 days. $CD4^{+}$ T cells were classified according to their proliferative response as "Proliferative" ($CFSE^{dim}$) or "Non-proliferative" ($CFSE^{bright}$). Memory subpopulations were analyzed (Naïve; central memory, CM; effector memory cells re-expressing CD45RA, EMRA; effector memory, EM). **(B)** Representative gating strategy to identify memory subpopulations in proliferative ($CFSE^{dim}$) and non-proliferative ($CFSE^{bright}$) SARS-CoV-2 Spike-specific $CD4^{+}$ T cells in sample 2 (left, 14 days after the second dose) and sample 3 (right, 230 days after the second dose). **(C)** Representative gating strategy to identify memory subpopulations in proliferative ($CFSE^{dim}$) and non-proliferative ($CFSE^{bright}$) SARS-CoV-2 Spike-specific $CD8^{+}$ T cells in sample 2 (left, 14 days after the second dose) and sample 3 (right, 230 days after the second dose).

Supplementary Figure 4

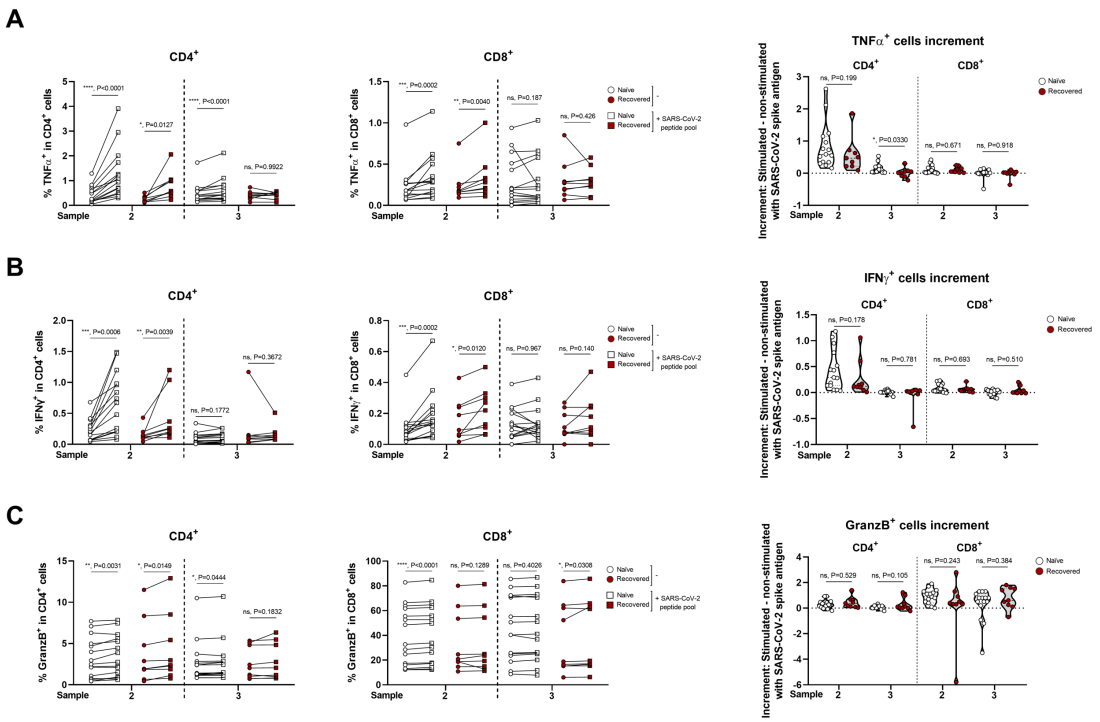

Figure S4. SARS-CoV-2 Spike protein-specific intracellular cytokines production by T cells from naïve and COVID-19-recovered individuals. Frequency of TNFα$^+$ (**A**), IFNγ$^+$ (**B**) and Granzyme-B$^+$ (**C**) CD4$^+$ (left panel) and CD8$^+$ (middle panel) T cells from naïve and COVID-19-recovered individuals, stimulated or not with a SARS-CoV-2 Spike peptide pool for 6 hours of sample 2 (14 days after second dose) and sample 3 (more than seven months after second dose). Increment of TNFα$^+$ **(A)**, IFNγ$^+$ **(B)** and Granzyme-B$^+$ **(C)** cells (right panels) comparing SARS-CoV-2 Spike pool-stimulated and non-stimulated CD4$^+$ and CD8$^+$ T cells from naïve and COVID-19-recovered individuals of sample 2 and sample 3. Each dot represents an individual. (Left and middle panels) Paired Student's test (ns, not significant; * P<0.05; **, P<0.01; ***, P<0.001; ****, P<0.0001). (Right panels) Mann Whitney test (ns, not significant; *, P<0.05)

Supplementary Figure 5

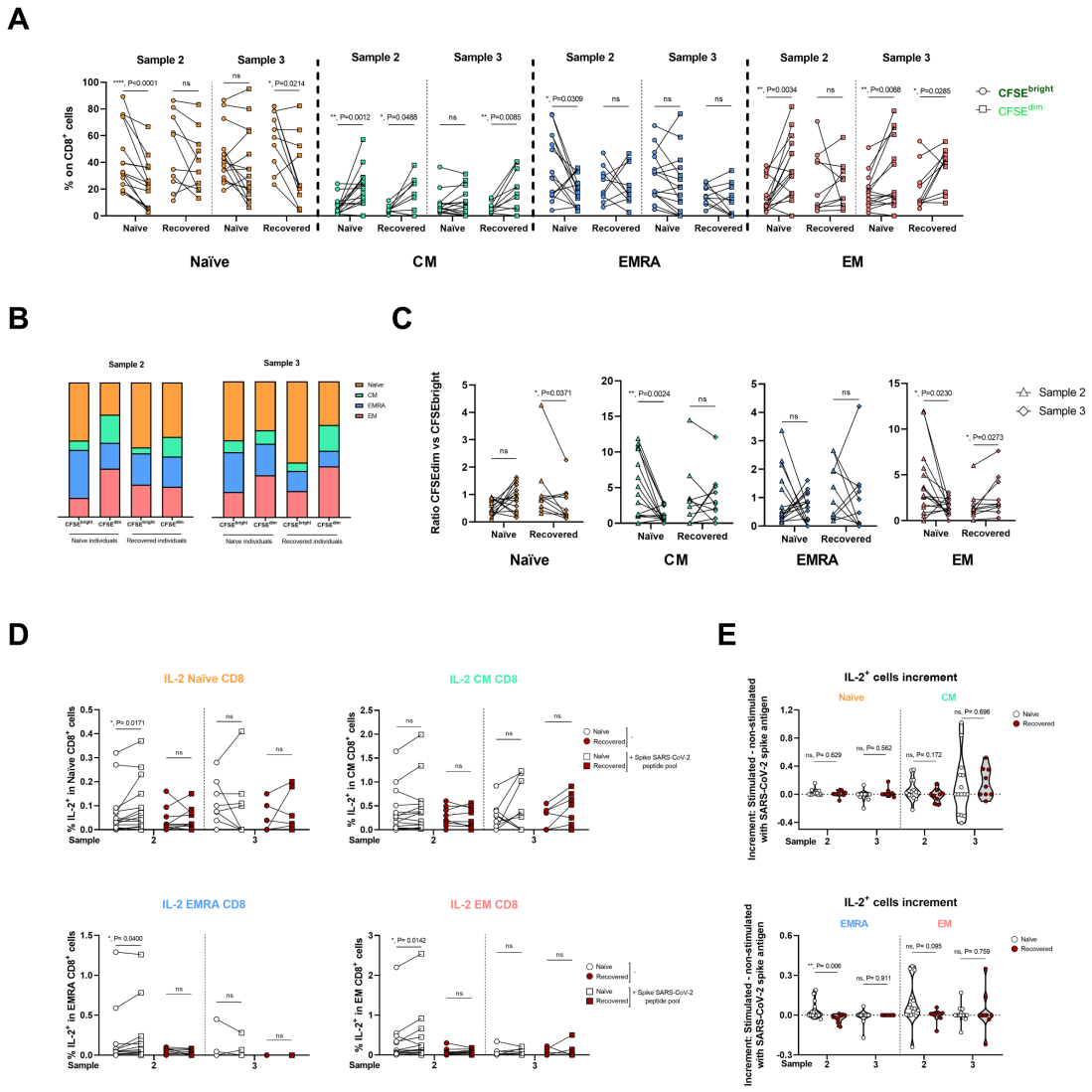

Figure S5. Memory populations in SARS-CoV-2 spike-specific CD8$^+$ T cells after BNT162b2 mRNA vaccination in naïve and COVID-19-recovered individuals. PBMCs were labelled with CFSE and stimulated with SARS-CoV-2 spike peptide pool for 5 days. CD8$^+$ T cells were classified according to their proliferative response as "Proliferative" (CFSE^{dim}) or "Non-proliferative" (CFSE^{bright}). Memory subpopulations were analyzed (Naïve; central memory, CM; effector memory cells re-expressing CD45RA, EMRA; effector memory, EM). Frequencies (**A**) and mean distribution (**B**) of memory populations in "Proliferative" (○, CFSE^{dim}) and non-proliferative (□, CFSE^{bright}) CD8$^+$ T cells from naïve and COVID-19-recovered individuals in sample 2 (14 days after second dose) and sample 3 (more than seven months after second dose). (**C**) "Proliferative" (CFSE^{dim}) versus "Non-proliferative" (CFSE^{bright}) ratio of CD8$^+$ T cell memory populations from naïve and COVID-19-recovered individuals in sample 2 (Δ) and sample 3 (◊). (**D**) Frequency of IL-2$^+$ cells in gated naïve, CM, EMRA and EM CD8$^+$ T cells stimulated or not with SARS-CoV-2 spike peptide pool for 6 hours in sample 2 and sample 3. (**E**) Increment of frequencies of IL-2$^+$ cells comparing SARS-CoV-2 spike pool-stimulated and non-stimulated CD8$^+$ T cell subpopulations, naïve and CM (upper panel), EMRA and EM (lower panel), from naïve and COVID-19-recovered individuals in sample 2 and sample 3. (A, C-E) Each dot represents an individual. (A, C-D) Paired Student's t-test (ns, not significant; *, P<0.05; **, P<0.01; ****, P<0.0001). (E) Mann Whitney t test (ns, not significant; **, P<0.01).

SUPPLEMENTARY TABLES

Table S1. Demographics and laboratory findings from naïve and COVID-19-recovered individuals

	All HVs (n=27)	Naïve (n=16)	Recovered (n=11)	P-value
Age – years	42.37±14.74	46.44±16.02	36.45±10.72	0.069
Sex, male – n (%)	10 (58.82)	5 (50.00)	5 (71.43)	0.484
Laboratory findings – n, (%)				
Red blood cells – Counts/cm^3	5260±690	5380±780	5080±510	0.5037
Haemoglobin – g/dL	15.68±2.13	15.78±2.34	15.53±1.89	0.8748
Haematocrit – (%)	48.87±6..67	49.66±7.42	47.72±5.54	0.9318
White-cells – Counts/cm^3	6.73±1.71	6.32±1.27	7.33±2.12	0.087
ALC – Counts/cm^3	2.29±0.68	2.18±0.77	2.44±0.52	0.107
ANC – Counts/cm^3	3.71±1.42	3.25±0.93	4.37±1.77	0.069
AMC – Counts/cm^3	0.38±0.10	0.37±0.10	0.40±0.11	0.761
AEC – Counts/cm^3	0.27±0.21	0.22±0.14	0.35±0.27	0.288
ABS – Counts/cm^3	0.07±0.02	0.06±0.02	0.08±0.02	0.056
Platelet counts	244.33±57.92	228.75±55.03	267.00±56.81	0.068
Ratio N/L	1.73±0.87	1.60±0.63	1.92.±1.14	0.8177

Data are expressed as mean±SD or number (percentage)

Table S2. List of all fluorochrome-conjugated monoclonal antibodies for flow cytometry analysis.

Marker	Fluorochrome	Source	Clone	Reference
CD45RA	BUV395	BD	5H9	Cat# 740315
CD16	BUV496	BD	3G8	Cat# 612944
CCR5	BUV563	BD	3A9	Cat# 741401
CD62L	BUV615	BD	SK11	Cat# 751364
CD11c	BUV661	BD	B-Ly6	Cat# 612967
CD56	BUV737	BD	NCAM 16.2	Cat# 612766
CD8	BUV805	BD	SK1	Cat# 612889
IgD	BV480	BD	IA6-2	Cat# 566138
IgG	BV605	BD	G18-145	Cat# 563246
CXCR5	BV750	BD	RF8B2	Cat# 747111
CD141	BB515	BD	1A4	Cat# 566017
CD127	APC-R700	BD	HIL-7R-M21	Cat# 565185
CD163	BB790	BD	GHI/61	Cat# 624296
NKG2C	BB700	BD	134591	BD OptiBuild
CD123	Super Bright 436	ThermoFisher Scientific	6H6	Cat# 62-1239-42
CD161	eFluor 450	ThermoFisher Scientific	HP-3G10	Cat# 48-1619-42
CD20	Pacific Orange	ThermoFisher Scientific	2H7	Cat# MHCD2030
TCRγδ	PerCP-eFluor 710	ThermoFisher Scientific	B1.1	Cat# 46-9959-42
CD25	PE-Alexa Fluor 700	ThermoFisher Scientific	CD25-3G10	Cat# MHCD2524
CCR7	BV421	Biolegend	G043H7	Cat# 353208
CD3	BV510	Biolegend	OKT3	Cat# 317332
IgM	BV570	Biolegend	MHM-88	Cat# 314517
CD28	BV650	Biolegend	CD28.2	Cat# 302946
CCR6	BV711	Biolegend	G034E3	Cat# 353436
PD-1	BV785	Biolegend	EH12.2H7	Cat# 329929
CD57	FITC	Biolegend	HNK-1	Cat# 359604
CD14	Spark Blue™ 550	Biolegend	63D3	Cat# 367148
CD45	PerCP	Biolegend	2D1	Cat# 368506
CD11b	PerCP/Cyanine5.5	Biolegend	ICRF44	Cat# 301328
PD-L1	PE	Biolegend	10F.9G2	Cat# 124308
CD24	PE/Dazzle™ 594	Biolegend	ML5	Cat# 311134
CD95	PE/Cy5	Biolegend	DX2	Cat# 305610
CXCR3	PE/Cy7	Biolegend	G025H7	Cat# 353720
CD27	APC	Biolegend	M-T271	Cat# 356410
CD1c	Alexa Fluor® 647	Biolegend	L161	Cat# 331510
CD19	Spark NIR™ 685	Biolegend	HIB19	Cat# 302270
HLA-DR	APC/Fire™ 750	Biolegend	L243	Cat# 307658
CD38	APC-Fire810	Biolegend	HIT2	Cat# 303550
CD4	cFluor-YG584	Cytek Biosciences	SK3	Cat# R7-20042

Table S3. List of fluorochrome-conjugated monoclonal antibodies for T cell proliferation assay by flow cytometry analysis

Marker	Fluorochrome	Source	Clone	Reference
CD3	BV510	Biolegend	OKT3	Cat# 317332
CD4	cFluor-YG584	Cytek Biosciences	SK3	Cat# R7-20042
CD8	BUV805	BD	SK1	Cat# 612889
CD45	PerCP	Biolegend	2D1	Cat# 368506
CD45RA	BUV395	BD	5H9	Cat# 740315
CD62L	BV615	BD	SK11	Cat# 751364
CD28	BV650	Biolegend	CD28.2	Cat# 302946
CCR7	BV421	Biolegend	G043H7	Car# 353208

Table S4. List of fluorochrome-conjugated monoclonal antibodies for extracellular and intracellular staining for T cell stimulation by flow cytometry analysis

Extracellular Marker	Fluorochrome	Source	Clone	Reference
CD3	BV570	Biolegend	UCHT1	Cat# 300436
CD4	PerCP/Cy5.5	Biolegend	SK3	Cat# 344608
CD8	BUV805	BD	SK1	Cat# 612889
CD45RA	BUV395	BD	5H9	Cat# 740315
CCR7	BUV737	BD	2-L1-A	Cat# 749676

Intracellular Marker	Fluorochrome	Source	Clone	Reference
Granzyme B	PE/Cy7	Biolegend	QA16A02	Cat# 372214
IFNγ	BV711	Biolegend	4S.B3	Cat# 502540
IL-2	APC-R700	BD	MQ1-17H12	Cat# 565136
TNFα	BV650	BD	MAb11	Cat# 563418